

Transformed Rank-1 Lattices for high-dimensional approximation

Robert Nasdala and Daniel Potts*

This paper describes an extension of Fourier approximation methods for multivariate functions defined on bounded domains to unbounded ones via a multivariate change of coordinate mapping. In this approach we adapt algorithms for the evaluation and reconstruction of multivariate trigonometric polynomials based on single and multiple reconstructing rank-1 lattices and make use of dimension incremental construction methods for sparse frequency sets. Various numerical tests confirm obtained theoretical results for the transformed methods.

Keywords and phrases : approximation on unbounded domains, change of coordinates, sparse multivariate trigonometric polynomials, lattice rule, multiple rank-1 lattice, fast Fourier transform

2010 AMS Mathematics Subject Classification : 65T 42B05

1 Introduction

The change of coordinates is a powerful tool in numerical analysis. Such transformations play an important role in spectral methods, numerical integration and approximation of functions. An excellent overview can be found in [1, Chapter 16 and 17] which contains many practical aspects of the mapped methods. In this paper we focus on change of coordinate mappings from multivariate bounded domains to unbounded ones in order to approximate functions defined on such unbounded domains. The main goal is to transfer the efficiency of Fourier methods on the high-dimensional torus \mathbb{T}^d to approximation methods on \mathbb{R}^d with the help of a transformation $\psi : \mathbb{T}^d \rightarrow \mathbb{R}^d$. Such a transformation induces a weighted scalar product

$$(f, g)_{L_{2,\psi}(\mathbb{R}^d)} = \int_{\mathbb{R}^d} (\psi^{-1}(\mathbf{y}))' f(\mathbf{y}) \overline{g(\mathbf{y})} d\mathbf{y},$$

with which we define transformed Fourier coefficients $\hat{h}_{\mathbf{k},\psi}$ and the transformed Fourier partial sum

$$S_I h(\mathbf{y}) = \sum_{\mathbf{k} \in I} \hat{h}_{\mathbf{k},\psi} e^{2\pi i \mathbf{k} \cdot \psi^{-1}(\mathbf{y})}$$

¹Technische Universität Chemnitz, Faculty of Mathematics, 09107 Chemnitz, Germany
robert.nasdala@math.tu-chemnitz.de, potts@math.tu-chemnitz.de

for a frequency set $I \subset \mathbb{Z}^d$. While the main question of Fourier approximation theory remains, that is, whether $S_I h$ converges to the original function h as the cardinality of I increases, we additionally have to take the particular choices of I and ψ into consideration.

On the other hand, one advantage of our method is the availability of fast algorithms, see e.g. [1], in contrast to approximation based on for instance multivariate Hermite functions or Sinc methods.

Another aspect we want to highlight are lattice rules that in recent years became an important tool in numerical analysis for high dimensional integration of multivariate functions. An introduction to lattice rules can be found in [14, 17, 5]. It was already pointed out that one can also use these rules for the approximation on the torus, see [19]. Recently efficient algorithms based on component-by-component methods [4, 3] were presented in order to compute high-dimensional integrals. For rank-1 lattices with M sampling points there are efficient algorithms for computing the discrete Fourier transforms [6], and furthermore these schemes provide good approximation properties, in particular for high-dimensional approximation problems, see [2]. We note that L. Kämmerer recently suggested to use multiple rank-1 lattices which are obtained by taking a union of several single rank-1 lattices, see [9, 8]. Using this method one can overcome the limitations of the single rank-1 lattice approach. That is, for the reconstruction of multivariate trigonometric polynomials supported on an arbitrary frequency set I of finite cardinality $|I| < \infty$ with a single reconstructing rank-1 lattice the lattice size M is bounded by $|I| \leq M \leq C|I|^2$ under mild assumptions, see e.g. [6, condition (3.2)]. Multiple rank-1 lattices improve the upper bound to $M \leq C|I| \log |I|$ with high probability. Remarkably, in both cases the upper bound is independent of the dimension d .

Furthermore we will use methods where the support of the transformed Fourier coefficients $\hat{h}_{\mathbf{k}, \psi}$ of the underlying function h is unknown. We adapt the methods presented in [15, 11] that describe a dimension incremental construction of a frequency set $I \subset \mathbb{Z}^d$ containing only non-zero or the approximately largest Fourier coefficients, based on component-by-component construction of rank-1 lattices. This will be done with respect to a specific search space in form of a full integer grid $[-N, N]^d \cap \mathbb{Z}^d$ with refinement $N \in \mathbb{N}$ and a sparsity that bounds the cardinality of the support.

The outline of the paper is as follows: In Section 2 we establish the basic notions from classical Fourier approximation theory on the torus, the corresponding function spaces and important convergence properties. Then we introduce the Wiener Algebra $\mathcal{A}_\omega(\mathbb{T}^d)$ as a function space in which the Fourier coefficients are absolutely summable. At last, we give the definition of rank-1 lattices as introduced in [12, 6] and discuss their importance in the context of Fourier approximation. Section 3 starts with the notion of a transformation $\psi : (-\frac{1}{2}, \frac{1}{2})^d \rightarrow \mathbb{R}^d$ that we easily extend onto the torus \mathbb{T}^d . Afterwards we combine them with the classical Fourier approximation theory, which causes the appearance of weighted scalar products and weighted functions spaces. A first major result appears in Lemma 3.3, where we show that a crucial upper approximation error bound still holds even after incorporating a transformation. We also introduce transformed rank-1 lattices as well as transformed multiple rank-1 lattices and discuss the relationship of the lattice size M and the cardinality of the frequency set $|I|$. On one hand, under mild assumptions we have $|I| \leq M \leq C|I|^2$ for a single rank-1 lattice, whereas the upper bound improves to $M \leq C|I| \log |I|$ with high probability for multiple rank-1 lattices. In Section 4 we provide and compare four particular examples for transformations ψ . In Section 5 we state our modified Algorithms for the evaluation and the reconstruction of transformed multivariate trigonometric polynomials, that are based on [6, Algorithm 3.1 and 3.2]. In Section 6 we pick up the error bound proved in Theorem 3.6

and highlight how the structure of the Wiener Algebra norm $\|\cdot\|_{\mathcal{A}_{\psi,\omega}(\mathbb{R}^d)}$ leads to a couple of appropriate choices for the frequency sets I . Afterwards we discuss how the choice of I affects the size of the Fourier matrices appearing in the Algorithms in Section 5 and their impact on the discretized approximation error. In Sections 7 and 8 we investigate various examples by composing the specific transformations from Section 4 with a particular test function. In some cases we can calculate the resulting transformed Fourier coefficients and are thus able to predetermine the frequency sets I for which the approximation error decays as proposed in Theorem 3.6. Additionally, we put our Algorithms 5.1 and 5.2 to the test and illustrate the resulting discrete approximation errors for an up to 12-dimensional test function h . In certain cases we additionally include multiple reconstructing rank-1 lattice algorithms and high-dimensional sparse fast Fourier algorithms.

2 Fourier approximation on the torus

First of all, we recall some definitions of classical Fourier approximation theory. Afterwards we introduce function spaces whose elements have absolute summable Fourier coefficients, so-called Wiener Algebras. Finally, we reflect the ideas of rank-1 lattices from [6], the references therein and their importance in the context of Fourier approximation.

2.1 Preliminaries

Let $\mathbb{T}^d \simeq [-\frac{1}{2}, \frac{1}{2}]^d$ be the d -dimensional torus. We define the function space $L_p(\mathbb{T}^d)$ for $1 \leq p < \infty$ as

$$L_p(\mathbb{T}^d) := \left\{ f : \mathbb{T}^d \rightarrow \mathbb{C} : \int_{\mathbb{T}^d} |f(\mathbf{x})|^p d\mathbf{x} < \infty \right\}$$

and for $p = \infty$ as

$$L_\infty(\mathbb{T}^d) := \left\{ f : \mathbb{T}^d \rightarrow \mathbb{C} : \text{ess sup}_{\mathbf{x} \in \mathbb{T}^d} |f(\mathbf{x})| < \infty \right\}.$$

Furthermore, $\mathcal{C}(\mathbb{T}^d)$ equipped with the L_∞ -norm is the collection of all continuous functions $f : \mathbb{T}^d \rightarrow \mathbb{C}$. Additionally, for functions f and g in the Hilbert space $L_2(\mathbb{T}^d)$ we have the scalar product

$$(f, g)_{L_2(\mathbb{T}^d)} = \int_{\mathbb{T}^d} f(\mathbf{x}) \overline{g(\mathbf{x})} d\mathbf{x}.$$

Later on we replace \mathbb{T}^d by \mathbb{R}^d in these definitions.

The functions $e^{2\pi i \mathbf{k} \cdot \circ}$, $\mathbf{k} \in \mathbb{Z}^d$, are orthogonal with respect to the L_2 -scalar product. By

$$\Pi_I := \text{span}\{e^{2\pi i \mathbf{k} \cdot \circ} : \mathbf{k} \in I\}$$

we denote the space of all multivariate trigonometric polynomials supported on the frequency set $I \subset \mathbb{Z}^d$ with finite cardinality $|I| < \infty$. For all $\mathbf{k} \in I$ we denote the *Fourier coefficients* $\hat{f}_{\mathbf{k}}$ by

$$\hat{f}_{\mathbf{k}} := (f, e^{2\pi i \mathbf{k} \cdot \circ})_{L_2(\mathbb{T}^d)} = \int_{\mathbb{T}^d} f(\mathbf{x}) e^{-2\pi i \mathbf{k} \cdot \mathbf{x}} d\mathbf{x},$$

and the corresponding *Fourier partial sum* by $S_I f(\mathbf{x}) := \sum_{\mathbf{k} \in I} \hat{f}_{\mathbf{k}} e^{2\pi i \mathbf{k} \cdot \mathbf{x}}$. The fact that Π_I is a dense subspace of $L_2(\mathbb{T}^d)$ implies that any $f \in \Pi_I$ is uniquely determined by the Fourier coefficients $(\hat{f}_{\mathbf{k}})_{\mathbf{k} \in I}$ such that $f(\mathbf{x}) = S_I f(\mathbf{x})$ and

$$\|f - S_I f\|_{L_2(\mathbb{T}^d)} \rightarrow 0 \quad \text{for } |I| \rightarrow \infty. \quad (2.1)$$

Here $|I| \rightarrow \infty$ means $\min(|k_1|, \dots, |k_d|) \rightarrow \infty$ for $\mathbf{k} = (k_1, \dots, k_d)^\top \in I$. In general, (2.1) is true for $f \in L_p(\mathbb{T}^d)$, $1 \leq p < \infty$, in the sense of $L_p(\mathbb{T}^d)$ -norm convergence, see [21, Theorem 4.1.].

2.2 Wiener Algebra

Every $f \in L_1(\mathbb{T}^d)$ with absolute summable Fourier coefficients has the continuous representative $\sum_{\mathbf{k} \in \mathbb{Z}^d} \hat{f}_{\mathbf{k}} e^{2\pi i \mathbf{k} \cdot \circ}$, which is shown in [6, Lemma 2.1.]. All such functions are collected in the *Wiener algebra*

$$\mathcal{A}_\omega(\mathbb{T}^d) := \left\{ f \in L_1(\mathbb{T}^d) : f(\mathbf{x}) = \sum_{\mathbf{k} \in \mathbb{Z}^d} \hat{f}_{\mathbf{k}} e^{2\pi i \mathbf{k} \cdot \mathbf{x}}, \sum_{\mathbf{k} \in \mathbb{Z}^d} \omega(\mathbf{k}) |\hat{f}_{\mathbf{k}}| < \infty \right\} \quad (2.2)$$

with $\omega : \mathbb{Z}^d \rightarrow [1, \infty]$ being some weight function. If $\omega(\mathbf{k}) = 1$ for all $\mathbf{k} \in \mathbb{Z}^d$ we write $\mathcal{A}(\mathbb{T}^d)$. In [6, Lemma 2.1.] it was also shown that

$$\mathcal{A}_\omega(\mathbb{T}^d) \subset \mathcal{A}(\mathbb{T}^d) \subset \mathcal{C}(\mathbb{T}^d).$$

A major problem we are going to discuss is how the frequency set $I \subset \mathbb{Z}^d$ needs to be chosen such that a function $f \in \mathcal{A}_\omega(\mathbb{T}^d)$ is approximated well by the Fourier partial sum $S_I f = \sum_{\mathbf{k} \in I} \hat{f}_{\mathbf{k}} e^{2\pi i \mathbf{k} \cdot \circ}$.

2.3 Rank-1 lattices and reconstructing rank-1 lattices

For each frequency set $I \subset \mathbb{Z}^d$ we define the *difference set*

$$\mathcal{D}(I) := \{\mathbf{k} \in \mathbb{Z}^d : \mathbf{k} = \mathbf{k}_1 - \mathbf{k}_2 \text{ with } \mathbf{k}_1, \mathbf{k}_2 \in I\}.$$

Furthermore, the set

$$\Lambda(\mathbf{z}, M) := \left\{ \mathbf{x}_j := \left(\frac{j}{M} \mathbf{z} \bmod \mathbf{1} \right) \in \mathbb{T}^d : j = 0, 1, \dots, M-1 \right\}$$

is called *rank-1 lattice* with the *generating vector* $\mathbf{z} \in \mathbb{Z}^d$, the *lattice size* $M \in \mathbb{N}$ and $\mathbf{1} := (1, \dots, 1)^\top \in \mathbb{Z}^d$. The *dual rank-1 lattice* is defined as

$$\Lambda(\mathbf{z}, M)^\perp := \left\{ \mathbf{k} \in \mathbb{Z}^d : \mathbf{k} \cdot \mathbf{z} \equiv 0 \pmod{M} \right\}.$$

A *reconstructing rank-1 lattice* $\Lambda(\mathbf{z}, M, I)$ is a rank-1 lattice $\Lambda(\mathbf{z}, M)$ for which the condition

$$\mathbf{t} \cdot \mathbf{z} \not\equiv 0 \pmod{M} \quad \text{for all } \mathbf{t} \in \mathcal{D}(I) \setminus \{\mathbf{0}\} \quad (2.3)$$

holds. $\Lambda(\mathbf{z}, M, I)^\perp$ denotes the *dual reconstructing rank-1 lattice* of $\Lambda(\mathbf{z}, M, I)$.

Given a reconstructing rank-1 lattice $\Lambda(\mathbf{z}, M, I)$, we have exact integration for all multivariate trigonometric polynomials $g \in \Pi_{\mathcal{D}(I)}$, see [18], such that

$$\int_{\mathbb{T}^d} g(\mathbf{x}) \, d\mathbf{x} = \frac{1}{M} \sum_{j=0}^{M-1} g(\mathbf{x}_j), \quad \mathbf{x}_j \in \Lambda(\mathbf{z}, M, I).$$

In particular, for $f \in \Pi_I$ and $\mathbf{k} \in I$ we have $f(\circ) e^{-2\pi i \mathbf{k} \cdot \circ} \in \Pi_{\mathcal{D}(I)}$ and

$$\hat{f}_{\mathbf{k}} = \int_{\mathbb{T}^d} f(\mathbf{x}) e^{-2\pi i \mathbf{k} \cdot \mathbf{x}} \, d\mathbf{x} = \frac{1}{M} \sum_{j=0}^{M-1} f(\mathbf{x}_j) e^{-2\pi i \mathbf{k} \cdot \mathbf{x}_j}, \quad \mathbf{x}_j \in \Lambda(\mathbf{z}, M, I). \quad (2.4)$$

On the other hand, for an arbitrary function $f \in \mathcal{A}_\omega(\mathbb{T}^d)$ and lattice points $\mathbf{x}_j \in \Lambda(\mathbf{z}, M, I)$ we lose the former mentioned exactness and get *approximated Fourier coefficients* $\hat{f}_{\mathbf{k}}^\Lambda$ of the form

$$\hat{f}_{\mathbf{k}} \approx \hat{f}_{\mathbf{k}}^\Lambda := \frac{1}{M} \sum_{j=0}^{M-1} f(\mathbf{x}_j) e^{-2\pi i \mathbf{k} \cdot \mathbf{x}_j} = \hat{f}_{\mathbf{k}} + \sum_{\mathbf{t} \in \Lambda(\mathbf{z}, M)^\perp \setminus \{\mathbf{0}\}} \hat{f}_{\mathbf{k}+\mathbf{t}}, \quad (2.5)$$

leading to the *approximated Fourier partial sum* $S_I^\Lambda f$ given by

$$S_I f(\mathbf{x}) \approx S_I^\Lambda f(\mathbf{x}) := \sum_{\mathbf{k} \in I} \hat{f}_{\mathbf{k}}^\Lambda e^{2\pi i \mathbf{k} \cdot \mathbf{x}}.$$

3 Fourier approximation on \mathbb{R}^d

Change of coordinate mappings were already discussed in [13] for high dimensional integration. In this chapter we describe the kind of transformations from \mathbb{T}^d to \mathbb{R}^d that we will use for high dimensional approximation. Then we introduce a variety of terms and objects a second time in their transformed version. This leads to Hilbert spaces with weighted norms, similar looking Wiener Algebras and the notion of transformed rank-1 lattices. However, even with an incorporated transformation a specific upper bound for the approximation error still holds.

3.1 Transformation to \mathbb{R}^d

We call a function $\psi : (-\frac{1}{2}, \frac{1}{2}) \rightarrow \mathbb{R}$ a *transformation* if it is continuously differentiable, increasing and we have

$$\lim_{x \rightarrow -\frac{1}{2}} \psi(x) = -\infty, \quad \lim_{x \rightarrow \frac{1}{2}} \psi(x) = \infty.$$

We denote its first derivative by $\psi' := d\psi/dx$. The respective inverse transformation is also continuously differentiable, increasing and is denoted by $\psi^{-1} : \mathbb{R} \rightarrow (-\frac{1}{2}, \frac{1}{2})$ in the sense of $y = \psi(x) \Leftrightarrow x = \psi^{-1}(y)$, so that

$$(\psi^{-1}(y))' = \frac{1}{\psi'(\psi^{-1}(y))}$$

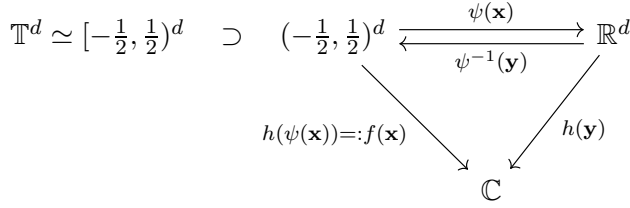


Figure 3.1: Scheme of the relation between f and h caused by a transformation ψ .

as well as $\lim_{y \rightarrow -\infty} \psi^{-1}(y) = -\frac{1}{2}$ and $\lim_{y \rightarrow \infty} \psi^{-1}(y) = \frac{1}{2}$. This implies $\|(\psi^{-1}(\cdot))'\|_{L_\infty(\mathbb{R})} < \infty$ and

$$\|(\psi^{-1}(\cdot))'\|_{L_1(\mathbb{R})} = \int_{-\infty}^{\infty} (\psi^{-1}(y))' dy = 1.$$

To get d -dimensional transformations we put $\psi(\mathbf{x}) := \psi(x_1, \dots, x_d) := (\psi(x_1), \dots, \psi(x_d))^\top$ and $\psi'(\mathbf{x}) := \psi'(x_1, \dots, x_d) := \prod_{j=1}^d \psi'(x_j)$, where we may use different maps in each direction.

3.2 Approximation of transformed functions

By $(\mathcal{C}_0(\mathbb{R}^d), \|\cdot\|_{L_\infty})$ we denote the space of all d -variate continuous functions vanishing at infinity. Considering a d -variate function $h \in L_1(\mathbb{R}^d)$, the composition of h with a transformation ψ yields a continuous and periodic function of the form

$$f(\mathbf{x}) := h(\psi(\mathbf{x})). \quad (3.1)$$

This is caused by ψ pushing h together onto the open cube $(-\frac{1}{2}, \frac{1}{2})^d$ and since h is vanishing in every direction, we put $h(\psi(\mathbf{x})) := 0$ for all boundary points $\mathbf{x} \in [-\frac{1}{2}, \frac{1}{2}]^d \setminus (-\frac{1}{2}, \frac{1}{2})^d$ in order to extend $h(\psi(\mathbf{x}))$ to $[-\frac{1}{2}, \frac{1}{2}]^d \simeq \mathbb{T}^d$, see Figure 3.1.

Based on the already established properties of periodic functions and the related approximation theory, we now use the premise in (3.1) that f and h can be transformed into one another in order to derive a similar terminology and approximation theory for functions $h \in L_1(\mathbb{R}^d)$. After resubstituting $\mathbf{x} = \psi^{-1}(\mathbf{y})$ we have transformed basis functions

$$\varphi_{\mathbf{k}}(\mathbf{y}) := e^{2\pi i \mathbf{k} \cdot \psi^{-1}(\mathbf{y})} \quad (\mathbf{k} \in \mathbb{Z}^d) \quad (3.2)$$

that span the space of all transformed multivariate trigonometric polynomials supported on $I \subset \mathbb{Z}^d$ with $|I| < \infty$, denoted by $\Pi_{I, \psi} := \text{span}\{e^{2\pi i \mathbf{k} \cdot \psi^{-1}(\cdot)} : \mathbf{k} \in I\}$. The system $(\varphi_{\mathbf{k}})_{\mathbf{k} \in \mathbb{Z}^d}$ is orthogonal on \mathbb{R}^d with respect to the weighted scalar product

$$(h_1, h_2)_{L_{2, \psi}(\mathbb{R}^d)} = \int_{\mathbb{R}^d} (\psi^{-1}(\mathbf{y}))' h_1(\mathbf{y}) \overline{h_2(\mathbf{y})} d\mathbf{y}$$

for $h_1, h_2 \in L_{2, \psi}(\mathbb{R}^d)$ with

$$L_{2, \psi}(\mathbb{R}^d) := \left\{ h : \mathbb{R}^d \rightarrow \mathbb{C} : \|h\|_{L_{2, \psi}(\mathbb{R}^d)} < \infty \right\}$$

being a weighted L_2 -space equipped with the induced norm $\|h\|_{L_2, \psi(\mathbb{R}^d)} = \sqrt{(h, h)_{L_2, \psi(\mathbb{R}^d)}}$. Hence, we have

$$(\varphi_{\mathbf{k}}, \varphi_{\mathbf{l}})_{L_2, \psi(\mathbb{R}^d)} = \delta_{\mathbf{k}, \mathbf{l}} \quad \text{for } \mathbf{k}, \mathbf{l} \in \mathbb{Z}^d.$$

Furthermore, we introduce the *transformed Fourier partial sum*

$$S_I h(\mathbf{y}) := \sum_{\mathbf{k} \in I} \hat{h}_{\mathbf{k}, \psi} e^{2\pi i \mathbf{k} \cdot \psi^{-1}(\mathbf{y})} \quad (3.3)$$

with *transformed Fourier coefficients* $\hat{h}_{\mathbf{k}, \psi}$ that are rewritten with respect to the weighted L_2 -scalar product, so that by (3.1) we observe

$$\begin{aligned} \hat{h}_{\mathbf{k}, \psi} &:= \int_{\mathbb{R}^d} (\psi^{-1}(\mathbf{y}))' h(\mathbf{y}) e^{-2\pi i \mathbf{k} \cdot \psi^{-1}(\mathbf{y})} d\mathbf{y} \\ &= \int_{\mathbb{T}^d} h(\psi(\mathbf{x})) e^{-2\pi i \mathbf{k} \cdot \mathbf{x}} d\mathbf{x} = \hat{f}_{\mathbf{k}}. \end{aligned} \quad (3.4)$$

Next we show that $\Pi_{I, \psi}$ is a dense subspace of $L_2, \psi(\mathbb{R}^d)$.

Lemma 3.1. *Let $\psi : (-\frac{1}{2}, \frac{1}{2})^d \rightarrow \mathbb{R}^d$ be a transformation and $I \subset \mathbb{Z}^d$ a frequency set of finite cardinality $|I| < \infty$. $\Pi_{I, \psi}$ is a dense subspace of $L_2, \psi(\mathbb{R}^d)$.*

Proof. Let ψ be a transformation, $I \subset \mathbb{Z}^d$ be an arbitrary frequency set of finite cardinality $|I| < \infty$ and $h \in \Pi_{I, \psi}$ a transformed multivariate trigonometric polynomial. Then there is a multivariate trigonometric polynomial $f \in \Pi_I$ such that $f(\mathbf{x}) = h(\psi(\mathbf{x}))$ for all $\mathbf{x} \in \mathbb{T}^d$ and the change of variables $\mathbf{y} = \psi(\mathbf{x})$ yields

$$\begin{aligned} \|h - S_I h\|_{L_2, \psi(\mathbb{R}^d)}^2 &= \int_{\mathbb{R}^d} (\psi^{-1}(y))' |h(\mathbf{y}) - S_I h(\mathbf{y})|^2 d\mathbf{y} \\ &= \int_{\mathbb{R}^d} (\psi^{-1}(y))' |h(\mathbf{y}) - \sum_{\mathbf{k} \in I} \hat{h}_{\mathbf{k}, \psi} e^{2\pi i \mathbf{k} \cdot \psi^{-1}(\mathbf{y})}|^2 d\mathbf{y} \\ &= \int_{\mathbb{T}^d} |f(\mathbf{x}) - \sum_{\mathbf{k} \in I} \hat{f}_{\mathbf{k}} e^{2\pi i \mathbf{k} \cdot \mathbf{x}}|^2 d\mathbf{x} \\ &= \|f - S_I f\|_{L_2(\mathbb{T}^d)}^2. \end{aligned}$$

Since $f \in \Pi_I \subset L_2(\mathbb{T}^d)$, we know that $\|f - S_I f\|_{L_2(\mathbb{T}^d)} \rightarrow 0$ for $|I| \rightarrow \infty$ in the sense of (2.1), so that $\Pi_{I, \psi}$ is dense in $L_2, \psi(\mathbb{R}^d)$. \blacksquare

3.3 Convergence criteria

Similar to (2.2) we now consider functions with absolutely summable weighted Fourier coefficients $\hat{h}_{\mathbf{k}, \psi} \in \mathbb{C}$ given in (3.4), so that $h(\mathbf{y}) = \sum_{\mathbf{k} \in \mathbb{Z}^d} \hat{h}_{\mathbf{k}, \psi} e^{2\pi i \mathbf{k} \cdot \psi^{-1}(\mathbf{y})}$ almost everywhere. These functions are collected in the *Wiener Algebra* $\mathcal{A}_{\psi, \omega}(\mathbb{R}^d)$, which is defined as

$$\mathcal{A}_{\psi, \omega}(\mathbb{R}^d) := \left\{ h \in L_1(\mathbb{R}^d) : h(\mathbf{y}) = \sum_{\mathbf{k} \in \mathbb{Z}^d} \hat{h}_{\mathbf{k}, \psi} e^{2\pi i \mathbf{k} \cdot \psi^{-1}(\mathbf{y})}, \|h\|_{\mathcal{A}_{\psi, \omega}(\mathbb{R}^d)} < \infty \right\}$$

with $\|h\|_{\mathcal{A}_{\psi,\omega}(\mathbb{R}^d)} := \sum_{\mathbf{k} \in \mathbb{Z}^d} \omega(\mathbf{k}) |\hat{h}_{\mathbf{k},\psi}|$ and the weight function $\omega : \mathbb{Z}^d \rightarrow [1, \infty]$. We simply write $\mathcal{A}_{\psi}(\mathbb{R}^d)$ if $\omega(\mathbf{k}) = 1$ for all $\mathbf{k} \in \mathbb{Z}^d$.

We now prove the existence of continuous representatives for functions $h \in \mathcal{A}_{\psi,\omega}(\mathbb{R}^d)$ and certain embeddings regarding the Wiener Algebra. We follow the arguments in [6, Lemma 2.1.], where the statement was shown for functions in $\mathcal{A}_{\omega}(\mathbb{T}^d)$.

Lemma 3.2. *Each $h \in \mathcal{A}_{\psi}(\mathbb{R}^d)$ has a continuous representative. Furthermore, we have the embeddings*

$$\mathcal{A}_{\psi,\omega}(\mathbb{R}^d) \subset \mathcal{A}_{\psi}(\mathbb{R}^d) \subset \mathcal{C}_0(\mathbb{R}^d).$$

Proof. Let $h \in \mathcal{A}_{\psi,\omega}(\mathbb{R}^d)$. We have $\omega(\mathbf{k}) \geq 1$ for all $\mathbf{k} \in \mathbb{Z}^d$ and estimate

$$\sum_{\mathbf{k} \in \mathbb{Z}^d} |\hat{h}_{\mathbf{k},\psi}| \leq \sum_{\mathbf{k} \in \mathbb{Z}^d} \omega(\mathbf{k}) |\hat{h}_{\mathbf{k},\psi}| < \infty,$$

so that $h \in \mathcal{A}_{\psi}(\mathbb{R}^d)$, too.

Now we show that $g := \sum_{\mathbf{k} \in \mathbb{Z}^d} \hat{h}_{\mathbf{k},\psi} e^{2\pi i \mathbf{k} \cdot \psi^{-1}(\cdot)}$ is a continuous representative of h . The sequence $(|\hat{h}_{\mathbf{k},\psi}|)_{\mathbf{k} \in \mathbb{Z}^d}$ is an ℓ_1 -sequence, hence, for all $\varepsilon > 0$ there exists an frequency set $I \subset \mathbb{Z}^d$ of finite cardinality with $\sum_{\mathbf{k} \in \mathbb{Z}^d \setminus I} |\hat{h}_{\mathbf{k},\psi}| < \frac{\varepsilon}{4}$. For a fixed $\mathbf{y}_0 \in \mathbb{R}^d$, we estimate

$$\begin{aligned} |g(\mathbf{y}_0) - g(\mathbf{y})| &= \left| \sum_{\mathbf{k} \in \mathbb{Z}^d} \hat{h}_{\mathbf{k},\psi} e^{2\pi i \mathbf{k} \cdot \psi^{-1}(\mathbf{y}_0)} - \sum_{\mathbf{k} \in \mathbb{Z}^d} \hat{h}_{\mathbf{k},\psi} e^{2\pi i \mathbf{k} \cdot \psi^{-1}(\mathbf{y})} \right| \\ &\leq \left| \sum_{\mathbf{k} \in I} \hat{h}_{\mathbf{k},\psi} e^{2\pi i \mathbf{k} \cdot \psi^{-1}(\mathbf{y}_0)} - \sum_{\mathbf{k} \in I} \hat{h}_{\mathbf{k},\psi} e^{2\pi i \mathbf{k} \cdot \psi^{-1}(\mathbf{y})} \right| + \frac{\varepsilon}{2}. \end{aligned}$$

The transformed multivariate trigonometric polynomial $S_I h(\mathbf{y}) = \sum_{\mathbf{k} \in I} \hat{h}_{\mathbf{k},\psi} e^{2\pi i \mathbf{k} \cdot \psi^{-1}(\mathbf{y})}$ is a continuous function. Accordingly, for $\varepsilon > 0$ and $\mathbf{y}_0 \in \mathbb{R}^d$ there exists $\delta_0 > 0$ such that $\|\mathbf{y}_0 - \mathbf{y}\|_1 < \delta_0$ implies $|S_I h(\mathbf{y}_0) - S_I h(\mathbf{y})| < \frac{\varepsilon}{2}$ and we obtain

$$|g(\mathbf{y}_0) - g(\mathbf{y})| < \varepsilon$$

for all \mathbf{y} with $\|\mathbf{y}_0 - \mathbf{y}\|_1 < \delta_0$. ■

This enables us to prove an adaptation of the crucial approximation error bound in [6, Lemma 2.2.] by using the same core arguments.

Lemma 3.3. *Let ψ be a transformation, $h \in \mathcal{A}_{\psi,\omega}(\mathbb{R}^d)$ and $I_N := \{\mathbf{k} \in \mathbb{Z}^d : \omega(\mathbf{k}) \leq N\}$ a frequency set of finite cardinality $|I_N| < \infty$. Then h can be approximated by the transformed Fourier partial sum*

$$S_{I_N} h(\mathbf{y}) = \sum_{\mathbf{k} \in I_N} \hat{h}_{\mathbf{k},\psi} e^{2\pi i \mathbf{k} \cdot \psi^{-1}(\mathbf{y})}$$

and the resulting approximation error can be estimated by

$$\|h - S_{I_N} h\|_{L^\infty(\mathbb{R}^d)} \leq \frac{1}{N} \|h\|_{\mathcal{A}_{\psi,\omega}(\mathbb{R}^d)}.$$

Proof. Let ψ be a transformation and $h \in \mathcal{A}_{\psi, \omega}(\mathbb{R}^d)$. Then $S_{I_N} h \in \mathcal{A}_{\psi, \omega}(\mathbb{R}^d) \subset \mathcal{C}_0(\mathbb{R}^d)$ and

$$\begin{aligned} \|h - S_{I_N} h\|_{L^\infty(\mathbb{R}^d)} &= \operatorname{ess\,sup}_{\mathbf{y} \in \mathbb{R}^d} |h(\mathbf{y}) - S_{I_N} h(\mathbf{y})| \\ &= \operatorname{ess\,sup}_{\mathbf{y} \in \mathbb{R}^d} \left| \sum_{\mathbf{k} \in \mathbb{Z}^d \setminus I_N} \hat{h}_{\mathbf{k}, \psi} e^{2\pi i \mathbf{k} \cdot \psi^{-1}(\mathbf{y})} \right| \\ &\leq \sum_{\mathbf{k} \in \mathbb{Z}^d \setminus I_N} |\hat{h}_{\mathbf{k}, \psi}| \leq \frac{1}{\inf_{\mathbf{k} \in \mathbb{Z}^d \setminus I_N} \omega(\mathbf{k})} \sum_{\mathbf{k} \in \mathbb{Z}^d \setminus I_N} \omega(\mathbf{k}) |\hat{h}_{\mathbf{k}, \psi}| \\ &\leq \frac{1}{N} \sum_{\mathbf{k} \in \mathbb{Z}^d} \omega(\mathbf{k}) |\hat{h}_{\mathbf{k}, \psi}| = \frac{1}{N} \|h\|_{\mathcal{A}_{\psi, \omega}(\mathbb{R}^d)}. \end{aligned}$$

■

3.4 Transformed rank-1 lattices

Next we adapt the idea of using reconstructing rank-1 lattices for functions $h \in \mathcal{A}_{\psi, \omega}(\mathbb{R}^d)$. Given a rank-1 lattice $\Lambda(\mathbf{z}, M)$ and a transformation ψ , the *transformed rank-1 lattice* $\Lambda_\psi(\mathbf{z}, M)$ is defined as

$$\Lambda_\psi = \Lambda_\psi(\mathbf{z}, M) := \{\mathbf{y}_j = \psi(\mathbf{x}_j) : \mathbf{x}_j \in \Lambda(\mathbf{z}, M), j = 0, \dots, M-1\}.$$

Accordingly, we denote the respective *transformed reconstructing rank-1 lattice* by $\Lambda_\psi(\mathbf{z}, M, I)$. For those there is the same exact integration property as in (2.4) for $f \in \Pi_I$. Given a transformed reconstructing rank-1 lattice $\Lambda_\psi(\mathbf{z}, M, I)$, we have exact integration for all multivariate trigonometric polynomials $h \in \Pi_{\mathcal{D}(I), \psi}$, such that

$$\int_{\mathbb{R}^d} (\psi^{-1}(\mathbf{y}))' h(\mathbf{y}) \, d\mathbf{y} = \frac{1}{M} \sum_{j=0}^{M-1} h(\mathbf{y}_j), \quad \mathbf{y}_j \in \Lambda_\psi(\mathbf{z}, M, I).$$

In particular, for $h \in \Pi_{I, \psi}$ and $\mathbf{k} \in I$ we have $h(\circ) e^{-2\pi i \mathbf{k} \cdot \psi^{-1}(\circ)} \in \Pi_{\mathcal{D}(I), \psi}$ and

$$\hat{h}_{\mathbf{k}, \psi} = \int_{\mathbb{R}^d} (\psi^{-1}(\mathbf{y}))' h(\mathbf{y}) e^{-2\pi i \mathbf{k} \cdot \psi^{-1}(\mathbf{y})} \, d\mathbf{y} = \frac{1}{M} \sum_{j=0}^{M-1} h(\mathbf{y}_j) e^{-2\pi i \mathbf{k} \cdot \psi^{-1}(\mathbf{y}_j)} \quad (3.5)$$

with $\mathbf{y}_j \in \Lambda_\psi(\mathbf{z}, M, I)$. However, for an arbitrary $h \in \mathcal{A}_{\omega, \psi}(\mathbb{R}^d)$ and transformed lattice points $\mathbf{y}_j \in \Lambda_\psi(\mathbf{z}, M, I)$ we lose the former mentioned exactness and get *approximated transformed Fourier coefficients* $\hat{h}_{\mathbf{k}, \psi}^\Lambda$ of the form

$$\hat{h}_{\mathbf{k}, \psi} \approx \hat{h}_{\mathbf{k}, \psi}^\Lambda := \frac{1}{M} \sum_{j=0}^{M-1} h(\mathbf{y}_j) e^{-2\pi i \mathbf{k} \cdot \psi^{-1}(\mathbf{y}_j)} = \frac{1}{M} \sum_{j=0}^{M-1} h(\psi(\mathbf{x}_j)) e^{-2\pi i \mathbf{k} \cdot \mathbf{x}_j}, \quad (3.6)$$

leading to the *approximated transformed Fourier partial sum* $S_{I_N}^\Lambda h$ given by

$$S_{I_N}^\Lambda h(\mathbf{y}) := \sum_{\mathbf{k} \in I_N} \hat{h}_{\mathbf{k}, \psi}^\Lambda e^{2\pi i \mathbf{k} \cdot \psi^{-1}(\mathbf{y})}. \quad (3.7)$$

The expression (3.6) can be rewritten further in the form of

$$\begin{aligned}
\hat{h}_{\mathbf{k},\psi}^{\Lambda} &= \frac{1}{M} \sum_{j=0}^{M-1} h(\psi(\mathbf{x}_j)) e^{-2\pi i \mathbf{k} \cdot \mathbf{x}_j} = \frac{1}{M} \sum_{j=0}^{M-1} \left(\sum_{\mathbf{t} \in \mathbb{Z}^d} \hat{h}_{\mathbf{t},\psi} e^{2\pi i \mathbf{t} \cdot \mathbf{x}_j} \right) e^{-2\pi i \mathbf{k} \cdot \mathbf{x}_j} \\
&= \frac{1}{M} \sum_{j=0}^{M-1} \sum_{\mathbf{t} \in \mathbb{Z}^d} \hat{h}_{\mathbf{t},\psi} e^{2\pi i (\mathbf{t}-\mathbf{k}) \cdot \mathbf{x}_j} = \sum_{\mathbf{t} \in \mathbb{Z}^d} \hat{h}_{\mathbf{t}+\mathbf{k},\psi} \left(\frac{1}{M} \sum_{j=0}^{M-1} e^{2\pi i \mathbf{t} \cdot \mathbf{x}_j} \right) \\
&= \sum_{\mathbf{t} \in \Lambda(\mathbf{z}, M)^\perp} \hat{h}_{\mathbf{t}+\mathbf{k},\psi}, \tag{3.8}
\end{aligned}$$

where the last equation is due to the fact that the lattice points lead to a geometric sum with

$$\frac{1}{M} \sum_{j=0}^{M-1} e^{2\pi i \mathbf{t} \cdot \mathbf{x}_j} = \begin{cases} 1 & \text{for } \mathbf{t} \in \Lambda(\mathbf{z}, M)^\perp \Leftrightarrow \mathbf{t} \cdot \mathbf{z} \equiv 0 \pmod{M}, \\ 0 & \text{otherwise.} \end{cases} \tag{3.9}$$

The next Lemma states that under mild assumptions the number of sampling points M of the reconstructing lattice rule is bounded above by the square of the cardinality of the frequency set I , see [6, condition (3.2)]. Hence, the length of a any such lattice rule does not become arbitrarily large and most importantly the upper bound is independent of the dimension d .

Lemma 3.4. *Let $I \subset \mathbb{Z}^d$ be a frequency set of finite cardinality $|I| < \infty$ with $I \subset [-|I|, |I|]^d$ and $|I| > 8$. For all transformed multivariate polynomials $h \in \Pi_{I,\psi}$ there exists a transformed reconstructing rank-1 lattice $\Lambda_\psi(\mathbf{z}, M, I)$ and a constant $C > 1$ such that the lattice size $M \in \mathbb{N}$ is bounded by $|I| \leq M \leq C|I|^2$ and*

$$\hat{h}_{\mathbf{k},\psi} = \frac{1}{M} \sum_{j=0}^{M-1} h(\mathbf{y}_j) e^{-2\pi i \mathbf{k} \cdot \psi^{-1}(\mathbf{y}_j)}, \quad \mathbf{y}_j \in \Lambda_\psi(\mathbf{z}, M, I).$$

Proof. The statement follows from combining [6, Corollary 3.4.] with the notions of transformed Fourier partial sums and transformed Fourier coefficients as in (3.3) and (3.4). ■

Furthermore, in [6, Lemma 3.10.] a certain relationship of a dual reconstructing rank-1 lattice $\Lambda(\mathbf{z}, M, I)^\perp$ and the frequency set $I \subset \mathbb{Z}^d$ was proven, which we use afterwards when proving error bounds for transformed Fourier approximations.

Lemma 3.5. *Let $I \subset \mathbb{Z}^d$ be a non-empty frequency set with $|I| < \infty$ such that $\Lambda(\mathbf{z}, M, I)$ is a reconstructing rank-1 lattice. Then*

$$\{\mathbf{k} + \mathbf{t} : \mathbf{k} \in I, \mathbf{t} \in \Lambda(\mathbf{z}, M, I)^\perp \setminus \{\mathbf{0}\}\} \subset \mathbb{Z}^d \setminus I$$

holds.

Proof. Suppose there are $\mathbf{k} \in I$ and $\mathbf{t} \in \Lambda(\mathbf{z}, M, I)^\perp \setminus \{\mathbf{0}\}$ such that $\mathbf{k} + \mathbf{t} \in I$. Then $\mathbf{0} \neq \mathbf{t} = (\mathbf{k} + \mathbf{t}) - \mathbf{k}$ is also an element of $\mathcal{D}(I)$. Since $\Lambda(\mathbf{z}, M, I)$ is a reconstructing rank-1 lattice for I , the fact that $\mathbf{t} \in \mathcal{D}(I) \cap \Lambda(\mathbf{z}, M, I)^\perp \setminus \{\mathbf{0}\}$ contradicts condition (2.3). ■

Now we prove an adaptation of another crucial approximation error bound in [6, Theorem 3.11.] by using the same core arguments for functions in the Wiener Algebra $\mathcal{A}_{\psi,\omega}(\mathbb{R}^d)$.

Theorem 3.6. *Let ψ be a transformation and $h \in \mathcal{A}_{\psi, \omega}(\mathbb{R}^d)$. Furthermore, for $N \in \mathbb{N}$ let $I_N = \{\mathbf{k} \in \mathbb{Z}^d : \omega(\mathbf{k}) \leq N\}$ be some non-empty frequency set with $|I_N| < \infty$ and let $\Lambda(\mathbf{z}, M, I_N)$ be a reconstructing rank-1 lattice.*

The approximation of h by the transformed approximated Fourier partial sum

$$S_{I_N}^\Lambda h(\mathbf{y}) = \sum_{\mathbf{k} \in I_N} \hat{h}_{\mathbf{k}, \psi}^\Lambda e^{2\pi i \mathbf{k} \cdot \psi^{-1}(\mathbf{y})}$$

leads to an approximation error that we can estimate by

$$\|h - S_{I_N}^\Lambda h\|_{L_\infty(\mathbb{R}^d)} \leq \frac{2}{N} \|h\|_{\mathcal{A}_{\psi, \omega}(\mathbb{R}^d)}. \quad (3.10)$$

Proof. With the triangle inequality we have

$$\|h - S_{I_N}^\Lambda h\|_{L_\infty(\mathbb{R}^d)} \leq \|h - S_{I_N} h\|_{L_\infty(\mathbb{R}^d)} + \|S_{I_N} h - S_{I_N}^\Lambda h\|_{L_\infty(\mathbb{R}^d)}.$$

In Lemma 3.3 we have already shown

$$\|h - S_{I_N} h\|_{L_\infty(\mathbb{R}^d)} \leq \frac{1}{N} \|h\|_{\mathcal{A}_{\omega, \psi}(\mathbb{R}^d)}.$$

For the other summand we use (3.8) to get

$$\begin{aligned} \|S_{I_N} h - S_{I_N}^\Lambda h\|_{L_\infty(\mathbb{R}^d)} &= \operatorname{ess\,sup}_{\mathbf{y} \in \mathbb{R}^d} \left| \sum_{\mathbf{k} \in I_N} \hat{h}_{\mathbf{k}, \psi} e^{2\pi i \mathbf{k} \cdot \psi^{-1}(\mathbf{y})} - \sum_{\mathbf{k} \in I_N} \hat{h}_{\mathbf{k}, \psi}^\Lambda e^{2\pi i \mathbf{k} \cdot \psi^{-1}(\mathbf{y})} \right| \\ &\leq \left| \sum_{\mathbf{k} \in I_N} \hat{h}_{\mathbf{k}, \psi}^\Lambda - \hat{h}_{\mathbf{k}, \psi} \right| \\ &= \sum_{\mathbf{k} \in I_N} \left| \left(\sum_{\mathbf{t} \in \Lambda(\mathbf{z}, M)^\perp} \hat{h}_{\mathbf{t} + \mathbf{k}, \psi} \right) - \hat{h}_{\mathbf{k}, \psi} \right| \\ &\leq \sum_{\mathbf{k} \in I_N} \sum_{\mathbf{t} \in \Lambda(\mathbf{z}, M)^\perp \setminus \{\mathbf{0}\}} |\hat{h}_{\mathbf{t} + \mathbf{k}, \psi}| \end{aligned}$$

and with Lemma 3.5 we can further estimate

$$\leq \sum_{\mathbf{k} \in \mathbb{Z}^d \setminus I_N} |\hat{h}_{\mathbf{k}, \psi}| \leq \frac{1}{\inf_{\mathbf{k} \in \mathbb{Z}^d \setminus I_N} \omega(\mathbf{k})} \sum_{\mathbf{k} \in \mathbb{Z}^d} \omega(\mathbf{k}) |\hat{h}_{\mathbf{k}, \psi}| = \frac{1}{N} \|h\|_{\mathcal{A}_{\psi, \omega}(\mathbb{R}^d)}.$$

■

3.5 Multiple transformed rank-1 lattices

In Lemma 3.4 it was shown that under mild assumptions we can construct a transformed reconstructing rank-1 lattice $\Lambda_\psi(\mathbf{z}, M, I)$ such that

$$|I| \leq M \leq C|I|^2$$

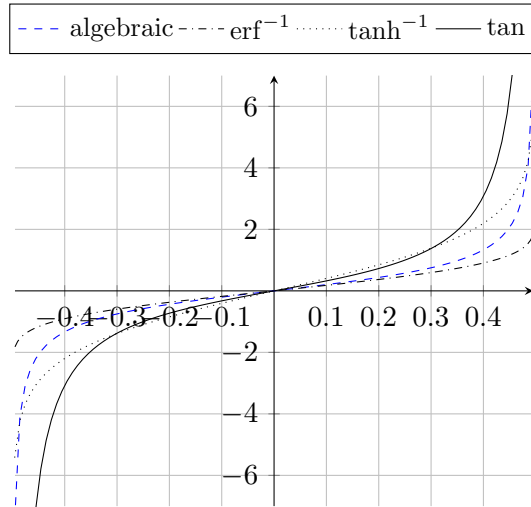


Figure 4.1: Plots of exemplary transformations ψ .

for a frequency set $I \subset \mathbb{Z}^d$ of finite cardinality $|I| < \infty$ and any transformed multivariate polynomial $h \in \Pi_{I,\psi}$. Even though this upper bound is independent of the dimension d , if the lattice size M is close to $|I|^2$ then it is still pretty large. In order to overcome this limitation of the single rank-1 lattice approach L. Kämmerer suggested the use of multiple rank-1 lattices which are obtained by taking a union of s rank-1 lattices $\Lambda(\mathbf{z}_1, M_1, \dots, \mathbf{z}_s, M_s)$, see [9, 8]. Then we can determine a reconstructing sampling set for multivariate trigonometric polynomials supported on the given frequency set I with a probability of at least $1 - \delta_s$, where

$$\delta_s = C_1 e^{-C_2 s}$$

is an upper bound on the probability that the approach fails and $C_1, C_2 > 0$ are constants. He furthermore proved that the upper bound on the lattice size improves with high probability to

$$M \leq C|I| \log |I|$$

for these particular reconstructing lattices. There are several other strategies in the literature to find appropriate reconstructing multiple rank-1 lattices, see [9, 8].

We are able to adapt this probabilistic approach for the former mentioned transformed rank-1 lattices and will later on show a particular example in which we construct transformed reconstructing multiple rank-1 lattices $\Lambda_\psi(\mathbf{z}_1, M_1, \dots, \mathbf{z}_s, M_s)$.

4 Examples for transformations

We list some feasible transformations ψ , see e.g. [1, Section 17.6] and [16, Section 7.5]. The definitions are made in one dimension and may contain a real parameter $c_j > 0$, that are collected in a vector $\mathbf{c} = (c_1, \dots, c_d)^\top$ when switching to the multivariate case. We simply write a single bold character \mathbf{c}_j if all entries c_j have the same value, e.g. $\mathbf{1} = (1, \dots, 1)^\top$.

Let $x \in (-\frac{1}{2}, \frac{1}{2})$ and $y \in \mathbb{R}$. We stress again that these change of coordinate mappings induce the transformed basis functions (3.2)

$$\varphi_k(y) = e^{2\pi i k \psi^{-1}(y)}, \quad k \in \mathbb{Z},$$

that form an orthogonal system such that

$$\int_{-\infty}^{\infty} (\psi^{-1}(y))' \varphi_k(y) \overline{\varphi_l(y)} dy = \delta_{k,l}, \quad k, l \in \mathbb{Z}.$$

We are particularly interested in the following transformations:

- *algebraic transformation:*

$$\psi(x) = c \frac{2x}{(1-4x^2)^{\frac{1}{2}}}, \quad \psi^{-1}(y) = \frac{y}{2(y^2+c^2)^{\frac{1}{2}}}, \quad (\psi^{-1}(y))' = \frac{c^2}{2(y^2+c^2)^{\frac{3}{2}}} \quad (4.1)$$

- *logarithmic transformation:*

$$\psi(x) = c \log \left(\frac{\frac{1}{2} + x}{\frac{1}{2} - x} \right) = 2c \tanh^{-1}(2x), \quad \psi^{-1}(y) = \frac{1}{2} \tanh \left(\frac{y}{2c} \right), \quad (4.2)$$

$$(\psi^{-1}(y))' = \frac{1}{4c} \left(1 - \tanh \left(\frac{y}{2c} \right)^2 \right)$$

- *error transformation:*

$$\psi(x) = c \operatorname{erf}^{-1}(2x), \quad \psi^{-1}(y) = \frac{1}{2} \operatorname{erf} \left(\frac{y}{c} \right), \quad (\psi^{-1}(y))' = \frac{1}{c\sqrt{\pi}} e^{-\left(\frac{y}{c}\right)^2} \quad (4.3)$$

with the error function

$$\operatorname{erf}(x) = \frac{1}{\sqrt{\pi}} \int_{-x}^x e^{-t^2} dt, \quad x \in \mathbb{R},$$

and $\operatorname{erf}^{-1}(\cdot)$ denoting the inverse error function.

- *tangens transformation:*

$$\psi(x) = c \tan(\pi x), \quad \psi^{-1}(y) = \frac{1}{\pi} \arctan \left(\frac{y}{c} \right), \quad (\psi^{-1}(y))' = \frac{1}{\pi} \left(\frac{c}{c^2 + y^2} \right) \quad (4.4)$$

For a side-by-side comparison of their individual velocity see Figure 4.1.

5 Algorithms

We compute the approximated transformed Fourier coefficients $\hat{h}_{\mathbf{k},\psi}^{\Lambda}$ given in (3.6) and the approximated Fourier series $S_{I_N}^{\Lambda} h$ given in (3.7) with slightly modified versions of two Algorithms found in [6, Algorithm 3.1 and 3.2] that are based on one-dimensional fast Fourier transforms (FFTs). In fact, we express the reconstruction and evaluation of a transformed multivariate trigonometric polynomial as the matrix-vector-products

$$\mathbf{h} = \mathbf{A} \hat{\mathbf{h}} \quad \text{and} \quad \hat{\mathbf{h}} = M^{-1} \mathbf{A}^* \mathbf{h} \quad (5.1)$$

with $\mathbf{h} = (h(\mathbf{y}_j))_{j=0,\dots,M-1}$, $\hat{\mathbf{h}} = (\hat{h}_{\mathbf{k}})_{\mathbf{k} \in I_N}$ and the transformed Fourier matrices \mathbf{A} and \mathbf{A}^* given by

$$\begin{aligned} \mathbf{A} &= \left(e^{2\pi i \mathbf{k} \cdot \psi^{-1}(\mathbf{y}_j)} \right)_{\mathbf{y}_j \in \Lambda_{\psi}(\mathbf{z}, M), \mathbf{k} \in I_N} \in \mathbb{C}^{M \times |I_N|}, \\ \mathbf{A}^* &= \left(e^{-2\pi i \mathbf{k} \cdot \psi^{-1}(\mathbf{y}_j)} \right)_{\mathbf{k} \in I_N, \mathbf{y}_j \in \Lambda_{\psi}(\mathbf{z}, M)} \in \mathbb{C}^{|I_N| \times M}. \end{aligned} \quad (5.2)$$

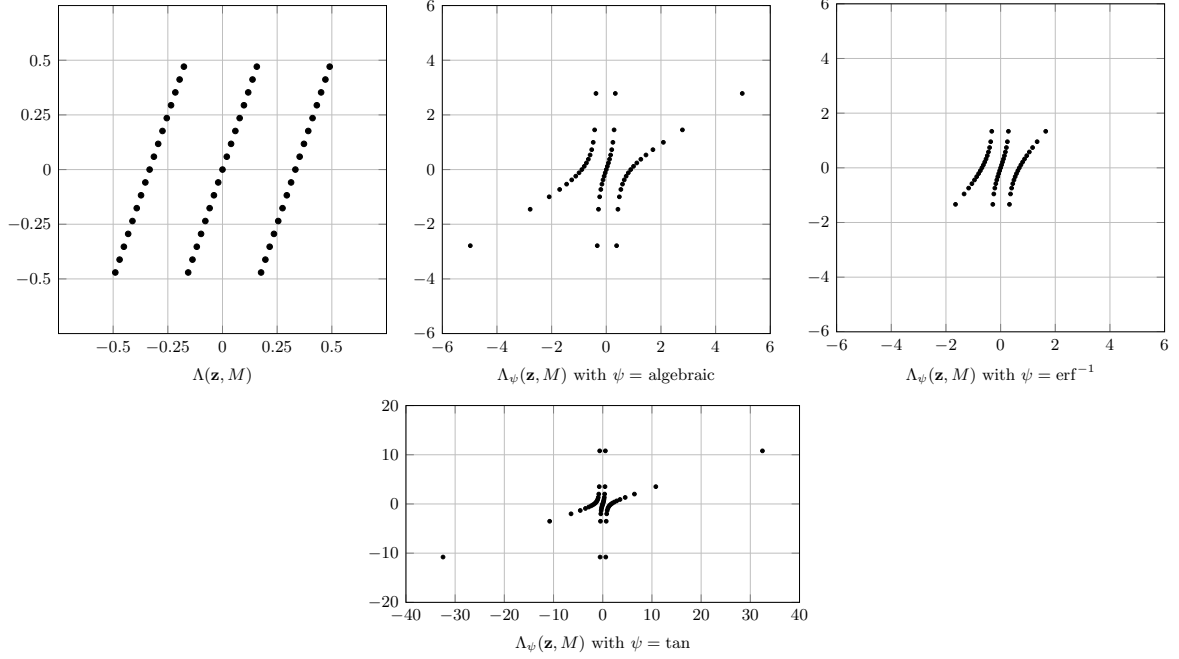


Figure 5.1: A two-dimensional lattice $\Lambda(\mathbf{z}, M)$ with $\mathbf{z} = (1, 3)^\top$, $M = 31$ and the corresponding transformed lattice $\Lambda_\psi(\mathbf{z}, M)$ with respect to the algebraic, the error and the tangens transformation and constants $\mathbf{c} = \mathbf{1}$.

5.1 Evaluation of transformed multivariate trigonometric polynomials

Algorithm 5.1 Evaluation at rank-1 lattice

Input:	$M \in \mathbb{N}$ $\mathbf{z} \in \mathbb{Z}^d$ $I \subset \mathbb{Z}^d$ $\hat{\mathbf{h}} = (\hat{h}_{\mathbf{k}})_{\mathbf{k} \in I}$	lattice size of $\Lambda_\psi(\mathbf{z}, M)$ generating vector of $\Lambda_\psi(\mathbf{z}, M)$ frequency set of finite cardinality Fourier coefficients of $h \in \Pi_{I, \psi}$
$\hat{\mathbf{g}} = (0)_{l=0}^{M-1}$ for each $\mathbf{k} \in I$ do $\hat{g}_{\mathbf{k} \cdot \mathbf{z} \bmod M} = \hat{g}_{\mathbf{k} \cdot \mathbf{z} \bmod M} + \hat{h}_{\mathbf{k}}$ end for $\mathbf{h} = \text{iFFT_1D}(\hat{\mathbf{g}})$ $\mathbf{h} = M\mathbf{h}$		
Output:	$\mathbf{h} = \mathbf{A}\hat{\mathbf{h}} = (h(\mathbf{y}_j))_{j=0}^{M-1}$	function values of $h \in \Pi_{I, \psi}$

Given a frequency set $I \subset \mathbb{Z}^d$ of finite cardinality $|I| < \infty$ we consider the transformed multivariate trigonometric polynomial $h \in \Pi_{I, \psi}$ with transformed Fourier coefficients $\hat{h}_{\mathbf{k}, \psi}$.

The evaluation of h at transformed lattice points $\mathbf{y}_j \in \Lambda_\psi(\mathbf{z}, M)$ simplifies to

$$h(\mathbf{y}_j) = \sum_{\mathbf{k} \in I} \hat{h}_{\mathbf{k}, \psi} e^{2\pi i \mathbf{k} \cdot \psi^{-1}(\mathbf{y}_j)} = \sum_{l=0}^{M-1} \left(\sum_{\substack{\mathbf{k} \in I, \\ \mathbf{k} \cdot \mathbf{z} \equiv l \pmod{M}}} \hat{h}_{\mathbf{k}, \psi} \right) e^{2\pi i l \frac{j}{M}} = \sum_{l=0}^{M-1} \hat{g}_l e^{2\pi i l \frac{j}{M}},$$

with

$$\hat{g}_l = \sum_{\substack{\mathbf{k} \in I, \\ \mathbf{k} \cdot \mathbf{z} \equiv l \pmod{M}}} \hat{h}_{\mathbf{k}, \psi}.$$

In order to evaluate h at the transformed lattice nodes \mathbf{y}_j , we simply pre-compute $(\hat{g}_l)_{l=0}^{M-1}$ and apply a one-dimensional inverse fast Fourier transform, see Algorithm 5.1.

5.2 Reconstruction of transformed multivariate trigonometric polynomials

Algorithm 5.2 Reconstruction from sampling values along a transformed reconstructing rank-1 lattice

Input:	$I \subset \mathbb{Z}^d$ $M \in \mathbb{N}$ $\mathbf{z} \in \mathbb{Z}^d$ $\mathbf{h} = (h(\mathbf{y}_j))_{j=0}^{M-1}$	frequency set of finite cardinality lattice size of $\Lambda_\psi(\mathbf{z}, M, I)$ generating vector of $\Lambda_\psi(\mathbf{z}, M, I)$ function values of $h \in \Pi_{I, \psi}$
--------	---	--

$\hat{\mathbf{g}} = \text{FFT_1D}(\mathbf{h})$

for each $\mathbf{k} \in I$ **do**

$$\hat{h}_{\mathbf{k}} = \frac{1}{M} \hat{g}_{\mathbf{k} \cdot \mathbf{z} \bmod M}$$

end for

Output:	$\hat{\mathbf{h}} = M^{-1} \mathbf{A}^* \mathbf{h} = (\hat{h}_{\mathbf{k}})_{\mathbf{k} \in I}$	Fourier coefficients supported on I
---------	---	---------------------------------------

For the reconstruction of a transformed multivariate trigonometric polynomial $h \in \Pi_{I, \psi}$ from transformed lattice points $\mathbf{y}_j \in \Lambda_\psi(\mathbf{z}, M, I)$ we utilize the exact integration property. Thus, by (3.4) and (3.5) we have

$$\hat{h}_{\mathbf{k}, \psi} = \int_{\mathbb{R}^d} (\psi^{-1}(\mathbf{y}))' h(\mathbf{y}) e^{-2\pi i \mathbf{k} \cdot \psi^{-1}(\mathbf{y})} d\mathbf{y} = \frac{1}{M} \sum_{j=0}^{M-1} h(\mathbf{y}_j) e^{-2\pi i \mathbf{k} \cdot \psi^{-1}(\mathbf{y}_j)}$$

for $\mathbf{y}_j \in \Lambda_\psi(\mathbf{z}, M, I)$ and also $\mathbf{A}^* \mathbf{A} = M\mathbf{I}$ with $\mathbf{I} \in \mathbb{C}^{|I| \times |I|}$ being the identity matrix. Hence, for the reconstruction of the transformed Fourier coefficients $\hat{h}_{\mathbf{k}, \psi}$ we use a single one-dimensional fast Fourier transform. The entries of the resulting vector $(\hat{g}_l)_{l=0}^{M-1}$ are renumbered by the means of the unique inverse mapping $\mathbf{k} \mapsto \mathbf{k} \cdot \mathbf{z} \bmod M$, see Algorithm 5.2.

6 The relation of frequency sets and reconstructing rank-1 lattices

We introduce two specific kinds of frequency sets I and discuss how the structure of the Wiener Algebra norm $\|\cdot\|_{\mathcal{A}_{\psi, \omega}(\mathbb{R}^d)}$ motivates these particular sets. Furthermore, we highlight how the choice of I impacts the size of the Fourier matrices \mathbf{A} and \mathbf{A}^* and ultimately the approximation error.

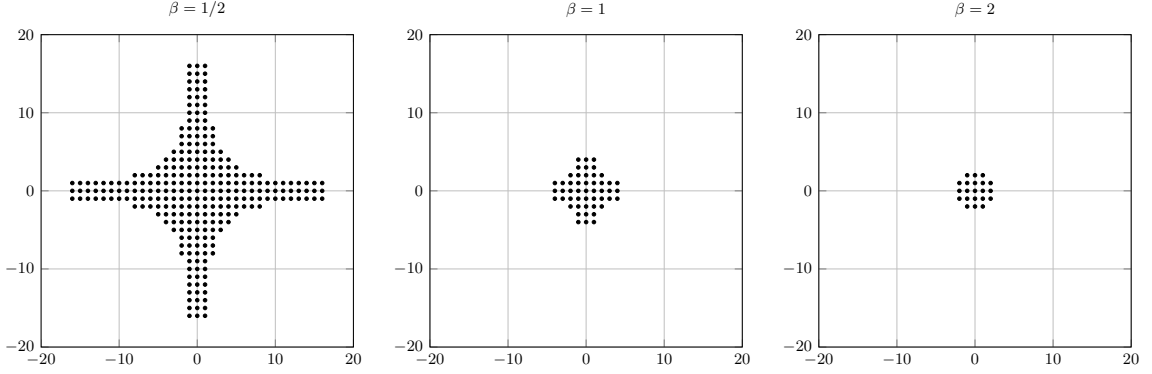


Figure 6.1: Two-dimensional hyperbolic crosses $I_N^{\text{hc},\beta}$ for $N = 4$ and $\beta = \frac{1}{2}, 1, 2$.

6.1 Hyperbolic crosses and discrete sequence spaces

For all $1 \leq p \leq \infty$ we denote the space of ℓ_p -summable d -dimensional integer sequences by $\ell_p \cap \mathbb{Z}^d$ and call it the *integer ℓ_p -space*. The respective integer unit ball of radius $N \in \mathbb{N}$ is defined as

$$I_N^{\ell_p} := \left\{ \mathbf{x} \in \mathbb{Z}^d : \|\mathbf{x}\|_p := \left(\sum_{j=1}^d |x_j|^p \right)^{\frac{1}{p}} \leq N \right\}.$$

Another frequently used frequency set is the *hyperbolic cross* $I_N^{\text{hc},\beta}$, defined as

$$I_N^{\text{hc},\beta} := \left\{ \mathbf{k} \in \mathbb{Z}^d : \omega_{\text{hc}}^\beta(\mathbf{k}) := \prod_{j=1}^d \max(1, |k_j|)^\beta \leq N \right\} \quad (6.1)$$

with $\beta > 0$ scaling the radius N , see Figure 6.1.

6.2 Finiteness of the upper error bounds

The choice of the frequency set is crucial for the development of the approximation error $\|h - S_{I_N}^\Delta h\|_{L^\infty(\mathbb{R}^d)}$ as $|I_N|$ increases. As proposed in (3.10), this error is bounded above by the Wiener algebra norm

$$\|h\|_{\mathcal{A}_{\psi,\omega}(\mathbb{R}^d)} = \sum_{\mathbf{k} \in \mathbb{Z}^d} \omega(\mathbf{k}) |\hat{h}_{\mathbf{k},\psi}|,$$

if I_N induces a reconstructing rank-1 lattice. On the other hand, this norm is finite if we have

$$\omega(\mathbf{k}) |\hat{h}_{\mathbf{k},\psi}| \lesssim \|\mathbf{k}\|_\infty^{-(1+\varepsilon)} \quad (6.2)$$

for $\min(|k_1|, \dots, |k_d|) \rightarrow \infty$ and $\varepsilon > 0$. Hence, the rate of decay of the $|\hat{h}_{\mathbf{k},\psi}|$ determines the range of feasible weight functions $\omega(\mathbf{k})$ and thus how the frequency set I_N needs to be shaped. In particular, for $I_N^{\text{hc},\beta}$ with $\omega_{\text{hc}}^\beta(\mathbf{k})$ the rate of decay of the transformed Fourier coefficients yields a range of values for β such that the Wiener algebra norm is finite.

I	$ I $	M	$ I /M$
$I_4^{\ell_\infty}$	81	81	1
$I_4^{\ell_{10}}$	53	60	0.8833
$I_4^{\ell_2}$	49	53	0.9245
$I_4^{\ell_1}$	41	44	0.9318
$I_4^{\text{hc},0.5}$	265	579	0.4577
$I_4^{\text{hc},1}$	49	58	0.8448
$I_4^{\text{hc},2}$	21	23	0.9130

Table 6.1: Comparison of the cardinality of various two-dimensional frequency sets of radius $N = 4$ and the sizes M of the respective reconstructing rank-1 lattices.

6.3 Discrete approximation error decay

We resort to the approximated Fourier coefficients $\hat{h}_{\mathbf{k},\psi}^\Lambda$, see (3.6), if we have no exact value of the $\hat{h}_{\mathbf{k},\psi}$ and discretize $\|h - S_I^\Lambda h\|_{L_\infty(\mathbb{R}^d)}$ so that it is evaluated at the set of transformed lattice points $\mathbf{y}_j \in \Lambda(\mathbf{z}, M)$. This discretization is based on the fact that we use Algorithm 5.1 to evaluate the vector $\mathbf{h} = (S_I^\Lambda h(\mathbf{y}_j))_{j=0,\dots,M-1}$ at transformed lattice points $\mathbf{y}_j \in \Lambda(\mathbf{z}, M)$, so that

$$\mathbf{h} = \mathbf{A}\hat{\mathbf{h}}, \quad \mathbf{A} \in \mathbb{C}^{M \times |I|}. \quad (6.3)$$

Based on the observation in (3.9), if $\Lambda(\mathbf{z}, M, I)$ is a reconstructing rank-1 lattice, then we have $\mathbf{A}^*\mathbf{A} = M\mathbf{I}$ for $|I| \leq M$ with $\mathbf{I} \in \mathbb{C}^{|I| \times |I|}$ being the identity matrix. Thus, for the inverse problem we use Algorithm 5.2 to evaluate

$$\hat{\mathbf{h}} = M^{-1}\mathbf{A}^*\mathbf{h}, \quad \mathbf{A}^* \in \mathbb{C}^{|I| \times M}. \quad (6.4)$$

Furthermore, in Lemma 3.4 it was shown under mild assumptions that for each frequency set I that induces a reconstructing rank-1 lattice, there is an $M \in \mathbb{N}$ such that $|I| \leq M \lesssim |I|^2$. On the other hand, $\mathbf{A}\mathbf{A}^* \in \mathbb{C}^{M \times M}$ is generally not an identity matrix. In particular for dimension $d = 2$ and radius $N = 4$, among the integer ℓ_p -unit balls with $1 \leq p \leq \infty$ and the hyperbolic crosses $I_N^{\text{hc},\beta}$ as introduced in (6.1), we only have an identity matrix for the ℓ_∞ -unit ball, see Table 6.1. Thus, in general we observe a gap between the initially given values \mathbf{h} and the resulting vector

$$\mathbf{h}_{\text{approx}} := M^{-1}\mathbf{A}\mathbf{A}^*\mathbf{h}$$

after applying Algorithms 5.2 and 5.1. We quantify such a gap with the *discrete approximation error* denoted by

$$\|\mathbf{h} - \mathbf{h}_{\text{approx}}\|_\infty, \quad (6.5)$$

or the *relative discrete approximation error* when considering the quotient $\|\mathbf{h} - \mathbf{h}_{\text{approx}}\|_\infty / \|\mathbf{h}\|_\infty$.

Depending on the particular choice of I , the error $\|\mathbf{h} - \mathbf{h}_{\text{approx}}\|_\infty$ doesn't necessarily converge to 0 for $M \rightarrow \infty$. In those cases we replace the Fourier partial sum and approximated

Fourier partial sum by the ℓ_q -Fejér mean, see [21, p. 20], that we define as

$$\sigma_{I_N}^q h(\mathbf{y}) := \sum_{\mathbf{k} \in I_N, \|\mathbf{k}\|_q \leq N} \left(1 - \frac{\|\mathbf{k}\|_q}{N}\right) \hat{h}_{\mathbf{k}, \psi} e^{2\pi i \mathbf{k} \cdot \psi^{-1}(\mathbf{y})},$$

and the respective approximated version given by

$$\sigma_{I_N}^{q, \Lambda} h(\mathbf{y}) := \sum_{\mathbf{k} \in I_N, \|\mathbf{k}\|_q \leq N} \left(1 - \frac{\|\mathbf{k}\|_q}{N}\right) \hat{h}_{\mathbf{k}, \psi}^\Lambda e^{2\pi i \mathbf{k} \cdot \psi^{-1}(\mathbf{y})}. \quad (6.6)$$

Even though the ℓ_q -Fejér means limit our choices for the frequency set I_N to ℓ_q -unit balls, the following Lemma found in [21, Lemma 6.2.] reveals their advantage over the classical Fourier partial sums.

Lemma 6.1. *Let $q \in \{1, \infty\}$ and $f \in L_p(\mathbb{T}^d)$ with $1 \leq p < \infty$ and $d \in \mathbb{N}$. Then*

$$\|f - \sigma_{I_N}^q f\|_{L_p(\mathbb{T}^d)} \rightarrow 0$$

for $\min(|k_1|, \dots, |k_d|) \rightarrow \infty$ with $\mathbf{k} = (k_1, \dots, k_d)^\top \in I_N$. This also holds for $q = 2$ if $d = 2$.

Remark 6.2. *Lemma 6.1 also holds for $q = 2$ in higher dimensions if we replace the ℓ_q -Fejér mean $\sigma_{I_N}^q f$ by the ℓ_q -Riesz mean $\sigma_{I_N}^{q, \alpha} f$ that is defined as*

$$\sigma_{I_N}^{q, \alpha} f(\mathbf{y}) := \sum_{\mathbf{k} \in I_N, \|\mathbf{k}\|_q \leq N} \left(1 - \left(\frac{\|\mathbf{k}\|_q}{N}\right)^\gamma\right)^\alpha \hat{f}_{\mathbf{k}} e^{2\pi i \mathbf{k} \cdot \psi^{-1}(\mathbf{y})}$$

with $0 < \alpha < \infty$ and $1 \leq \gamma < \infty$. Then Lemma 6.1 is true for $q = 2$ if $\alpha > (d - 1)/2$.

Another consequence of using ℓ_q -Fejér means is the change of the matrix-vector-product in Algorithm 5.1 into

$$(\sigma_{I_N}^\Lambda h(\mathbf{y}_j))_{j=0, \dots, M-1} = \mathbf{A} \mathbf{D}_\sigma \hat{\mathbf{h}} \quad \text{with} \quad \mathbf{D}_\sigma := \text{diag}((1 - \|\mathbf{k}\|_q/N)_{\mathbf{k} \in I_N}).$$

Hence, the combination of Algorithm 5.2 and Algorithm 5.1 leads to

$$\mathbf{h} \approx \mathbf{h}_{\text{approx}}^\sigma := M^{-1} \mathbf{A} \mathbf{D}_\sigma \mathbf{A}^* \hat{\mathbf{h}} \in \mathbb{C}^M.$$

and the *discrete Fejér approximation error* denoted by

$$\|\mathbf{h} - \mathbf{h}_{\text{approx}}^\sigma\|_\infty. \quad (6.7)$$

7 Examples

We choose

$$h(\mathbf{y}) = \prod_{j=1}^d \frac{1}{1 + y_j^2}, \quad (7.1)$$

as our test function, which according to [1, pp. 363-364] is rather difficult to approximate by classical approximation methods. We use the exemplary transformations (4.1)-(4.4) to put our Algorithms 5.1 and 5.2 to the test.

7.1 Algebraic transformation

We consider the algebraic transformation $\psi(\mathbf{x}) = \left(\frac{2x_1}{(1-4x_1^2)^{\frac{1}{2}}}, \dots, \frac{2x_d}{(1-4x_d^2)^{\frac{1}{2}}} \right)^\top$ with $\mathbf{c} = \mathbf{1}$, see (4.1). Then the transformed Fourier coefficients of h in (7.1) read as

$$\begin{aligned} \hat{h}_{\mathbf{k},\psi} &= \int_{\mathbb{R}^d} (\psi^{-1}(\mathbf{y}))' h(\mathbf{y}) e^{-2\pi i \mathbf{k} \cdot \psi^{-1}(\mathbf{y})} d\mathbf{y} = \int_{\mathbb{T}^d} h(\psi(\mathbf{x})) e^{-2\pi i \mathbf{k} \cdot \mathbf{x}} d\mathbf{x} \\ &= \int_{\mathbb{T}^d} \left(\prod_{j=1}^d \frac{1}{1 + \psi(x_j)^2} \right) e^{-2\pi i \mathbf{k} \cdot \mathbf{x}} d\mathbf{x} = \prod_{j=1}^d \int_{-1/2}^{1/2} \frac{e^{-2\pi i k_j x_j}}{1 + \frac{4x_j^2}{1-4x_j^2}} dx_j \\ &= \prod_{j=1}^d \int_{-1/2}^{1/2} (1 - 4x_j^2) e^{-2\pi i k_j x_j} dx_j \end{aligned}$$

with

$$\int_{-1/2}^{1/2} (1 - 4x_j^2) e^{-2\pi i k_j x_j} dx_j = \begin{cases} \frac{2}{3} & \text{for } k_j = 0, \\ \frac{2}{\pi^2} \frac{(-1)^{1+k_j}}{k_j^2} & \text{for } k_j \neq 0. \end{cases}$$

By recalling the argument related to condition (6.2) it becomes apparent that choosing I_N to be a hyperbolic cross $I_N^{\text{hc},\beta}$ as defined in (6.1) with $0 < \beta < 1$ yields a finite approximation error bound that was proven in Theorem 3.6, such that

$$\|h - S_{I_N^{\text{hc},\beta}}^\Lambda h\|_{L^\infty(\mathbb{R}^d)} \leq \frac{2}{N} \|h\|_{\mathcal{A}_{\psi,\omega}(\mathbb{R}^d)} = \frac{2}{N} \sum_{\mathbf{k} \in \mathbb{Z}^d} \omega_{\text{hc}}^\beta(\mathbf{k}) |\hat{h}_{\mathbf{k},\psi}| < \infty.$$

However, the rate of convergence slows down and the constant in the upper bound gets bigger the closer β is to 1.

As for the discrete approximation error (6.5) we apply Algorithms 5.1 and 5.2 as described in (6.3) and (6.4). We consider dimensions $d = 2, 3, 4, 5$ and the frequency set $I_N = I_N^{\text{hc},0.95}$ with $\beta = 0.95$ being an arbitrary choice. The radius $N \in \mathbb{N}$ ranges in a set of natural numbers $\{N_{\min}, \dots, N_{\max}\}$. We fix $N_{\min} = 2$ for all d , whereas the values of $N_{\max} \in \{120, 60, 30, 18\}$ are chosen individually and get smaller for higher dimensions. Depending on the particular N , we construct \mathbf{z} and M such that $\Lambda_\psi(\mathbf{z}, M, I_N^{\text{hc},0.95})$ is a transformed reconstructing rank-1 lattice. Then we form the initial vector $\mathbf{h} = (h(\mathbf{y}_j))_{j=0,\dots,M-1}$ with $\mathbf{y}_j \in \Lambda_\psi(\mathbf{z}, M, I_N^{\text{hc},0.95})$ and apply Algorithm 5.2 and Algorithm 5.1, yielding the vector $\mathbf{h}_{\text{approx}} = (S_{I_N}^\Lambda h(\mathbf{y}_j))_{j=0,\dots,M-1}$. For all considered dimensions d and increasing values of $N \in \mathbb{N}$ we indeed observe a relative discrete error decay of

$$\|\mathbf{h} - \mathbf{h}_{\text{approx}}\|_\infty \lesssim N^{-1},$$

showcased in the left plot of Figure 7.1.

We achieve similar results for the same input data when applying the multiple rank-1 algorithms described in [9, 8]. In particular we adapted [8, Algorithm 6]. Initializing this Algorithm with the parameters $c = 30, n = 30$ and $\delta = 0.5$ sustains the linear decay of the discrete approximation errors in all dimensions as seen in the right plot of Figure 7.1.

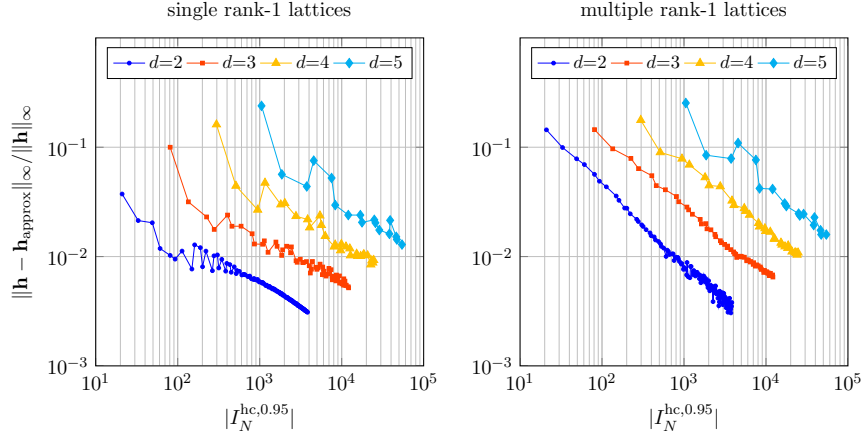


Figure 7.1: Relative discrete approximation error $\|\mathbf{h} - \mathbf{h}_{\text{approx}}\|_{\infty} / \|\mathbf{h}\|_{\infty}$ with single rank-1 lattices (left) and multiple rank-1 lattices (right) for the algebraic transformation and $I_N = I_N^{\text{hc},0.95}$.

7.2 Logarithmic and error transformation

By combining the same test function h as in (7.1) with the multivariate parametrized logarithmic function (4.2)

$$\psi(\mathbf{x}) = (2c_1 \tanh^{-1}(2x_1), \dots, 2c_d \tanh^{-1}(2x_d))^{\top}$$

we have

$$f(\mathbf{x}) = h(\psi(\mathbf{x})) = \prod_{j=1}^d \frac{1}{1 + (2c_j \tanh^{-1}(2x_j))^2}$$

with the transformed Fourier coefficients

$$\hat{h}_{\mathbf{k},\psi} = \prod_{j=1}^d \int_{-1/2}^{1/2} \frac{e^{-2\pi i k_j x_j}}{1 + (2c_j \tanh^{-1}(2x_j))^2} dx_j. \quad (7.2)$$

This time we don't know if there is a closed form for the transformed Fourier coefficients and therefore can't predetermine appropriate choices for I_N and \mathbf{c} in order to achieve the exact error decay as proposed in Theorem 3.6.

Nevertheless, we use this transformation to compare the decay of the discrete approximation error $\|\mathbf{h} - \mathbf{h}_{\text{approx}}\|_{\infty}$ to the discrete Fejér approximation error $\|\mathbf{h} - \mathbf{h}_{\text{approx}}^{\sigma}\|_{\infty}$ that we get after switching to the ℓ_q -Fejér means $\sigma_{I_N}^{q,\Lambda} h$, see (6.6) and (6.7). Additionally we use several constants $\mathbf{c} \in \{\frac{1}{2}, \mathbf{1}, \frac{3}{2}\}$ to show their impact on the approximation error. We fix the dimension $d = 2$ and the frequency sets $I_N \in \{I_N^{\ell_1}, I_N^{\ell_2}\}$. At first we look at $I_N = I_N^{\ell_1}$. Both relative discrete approximation errors $\|\mathbf{h} - \mathbf{h}_{\text{approx}}\|_{\infty} / \|\mathbf{h}\|_{\infty}$ and $\|\mathbf{h} - \mathbf{h}_{\text{approx}}^{\sigma}\|_{\infty} / \|\mathbf{h}\|_{\infty}$ decrease linearly for $N \rightarrow \infty$ as seen in the left column of Figure 7.2. The first row of the same Figure also showcases the much bigger difference in the error developments for $I_N^{\ell_2}$ compared to the error developments for $I_N^{\ell_1}$. Even though the observed rapid oscillation could just be

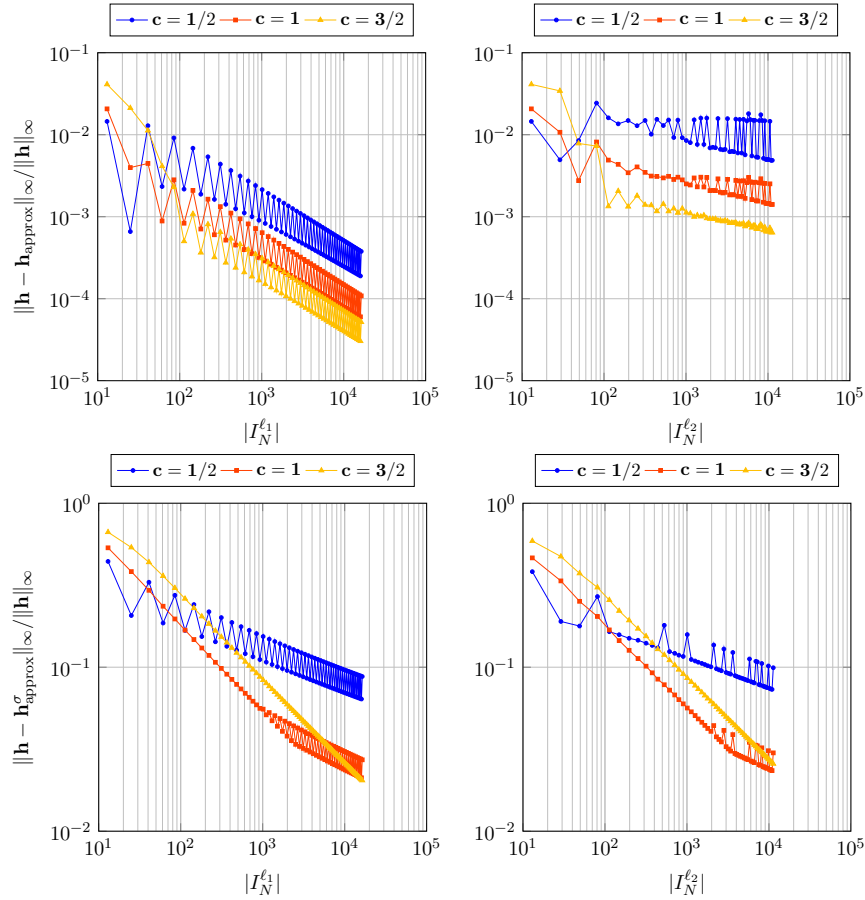


Figure 7.2: Comparison of the relative discrete approximation errors $\|\mathbf{h} - \mathbf{h}_{\text{approx}}\|_{\infty} / \|\mathbf{h}\|_{\infty}$ (top row) and relative discrete Fejér approximation error $\|\mathbf{h} - \mathbf{h}_{\text{approx}}^{\sigma}\|_{\infty} / \|\mathbf{h}\|_{\infty}$ (bottom row) in dimension $d = 2$ with the logarithmic transformation, $\mathbf{c} = \{\frac{1}{2}, \mathbf{1}, \frac{3}{2}\}$ and $I_N = I_N^{\ell_1}$ for $N = 2, 3, \dots, 100$ (left column) as well as $I_N = I_N^{\ell_2}$ for $N = 2, 3, \dots, 60$ (right column).

a result of how \mathbf{z} and M are chosen before the construction of the transformed rank-1 lattice and thus could be fixed by a different approach to choose them, the overall error decay of $\|\mathbf{h} - \mathbf{h}_{\text{approx}}\|_{\infty}$ is way slower for $I_N^{\ell_2}$. However, when switching to ℓ_q -Fejér means the error decay of $\|\mathbf{h} - \mathbf{h}_{\text{approx}}^{\sigma}\|_{\infty}$ looks much more like the ℓ_1 -unit ball one, illustrated for the relative errors in the bottom row of Figure 7.2

For the error transformation (4.3) we have the same problem of not having a closed form for the transformed Fourier coefficients. However, the numerical tests yield similar looking error decays as in Figure 7.2.

7.3 Tangens transformation

Considering the tangens transformation $\psi(\mathbf{x}) = (\tan(\pi x_1), \dots, \tan(\pi x_d))^\top$ with $\mathbf{c} = \mathbf{1}$, see (4.4), the one-dimensional transformed Fourier coefficients of the test function (7.1) read as

$$\hat{h}_{k_j, \psi} = \int_{-1/2}^{1/2} \frac{e^{-2\pi i k_j x_j}}{1 + \tan(\pi x_j)^2} dx_j = \int_{-1/2}^{1/2} \cos(\pi x_j)^2 e^{-2\pi i k_j x_j} dx_j = \begin{cases} \frac{1}{2} & \text{for } k_j = 0, \\ \frac{1}{4} & \text{for } |k_j| = 1, \\ 0 & \text{otherwise.} \end{cases} \quad (7.3)$$

They are bounded from above by

$$\hat{h}_{k_j, \psi} \leq \frac{1}{4} \left(\frac{1}{|k_j|} \right)^\alpha$$

for $k_j \neq 0$ and $\alpha > 0$, so that we have equality for $|k_j| = 1$ and an arbitrarily fast decay of $(|k_j|^{-\alpha})_{k_j \in \mathbb{Z}}$ for $|k_j| \rightarrow \infty$. Then for all $\beta > 0$ the hyperbolic cross $I_N^{\text{hc}, \beta}$ yields a finite approximation error in the form of

$$\|h - S_{I_N^{\text{hc}, \beta}}^\Lambda h\|_{L^\infty(\mathbb{R}^d)} \leq \frac{2}{4^d N} \sum_{\mathbf{k} \in \mathbb{Z}^d} \omega_{\text{hc}}^\beta(\mathbf{k}) |\hat{h}_{\mathbf{k}, \psi}| < \infty, \quad (7.4)$$

because for all arbitrarily large $\alpha > 1$ there is a $\beta > 0$ such that $\omega_{\text{hc}}^\beta(\mathbf{k}) |\hat{h}_{\mathbf{k}, \psi}| \sim \|\mathbf{k}\|_\infty^{-(\alpha-\beta)}$ with $\alpha - \beta > 1$ fulfills condition (6.2).

For certain transformations ψ the one-dimensional transformed Fourier coefficients $|\hat{h}_{k, \psi}|$ are of the form $b^{-|k|}$ with some real $b > 1$. In such cases they have the following estimate:

Lemma 7.1. *For all real $b > 1, \varepsilon > 0$ and $k \in \mathbb{N}$ there is a constant C , independent of k , such that*

$$b^{-k} \leq C k^{-1-\varepsilon}. \quad (7.5)$$

Proof. We consider $0 < k \in \mathbb{R}$ and $f(k) := b^{-k} k^{1+\varepsilon}$. Then its first derivative $f'(k) = b^{-k} k^\varepsilon ((1+\varepsilon) - k \log(b))$ has zeros at $k_1 = 0$ and $k_2 = \frac{1+\varepsilon}{\log(b)}$, and f has a maximum at k_2 . Hence, for all natural k the desired constant is given by

$$C = f(k_2) = b^{-\left(\frac{1+\varepsilon}{\log(b)}\right)} \left(\frac{1+\varepsilon}{\log(b)} \right)^{-(1+\varepsilon)}.$$

■

In case of the tangens transformation (4.4) with $0 < c_j \neq 1$, we have

$$\hat{h}_{k_j, \psi} = \int_{-1/2}^{1/2} \frac{e^{-2\pi i k_j x_j}}{1 + c_j^2 \tan(\pi x_j)^2} dx_j = \begin{cases} \frac{1}{c_j + 1} & \text{for } k_j = 0, \\ \frac{c_j}{(c_j + 1)^2} \left(\frac{c_j - 1}{c_j + 1} \right)^{|k_j|-1} & \text{for } k_j \neq 0. \end{cases} \quad (7.6)$$

For $c_j > 0$ we estimate $c_j(c_j + 1)^{-2} \leq 1/4$ and $b^{-1} := (c_j - 1)(c_j + 1)^{-1} < 1$, so that the estimate in (7.5) yields

$$\hat{h}_{k_j, \psi} \leq \frac{1}{4} C |k_j|^{-1-\varepsilon}.$$

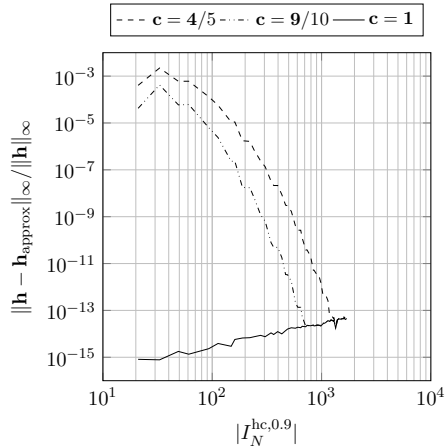


Figure 7.3: Relative discrete approximation error $\|\mathbf{h} - \mathbf{h}_{\text{approx}}\|_{\infty} / \|\mathbf{h}\|_{\infty}$ with $\psi(\mathbf{x}) = \mathbf{c} \tan(\pi \mathbf{x})$, $\mathbf{c} = \{\frac{4}{5}, \frac{9}{10}, \mathbf{1}\}$ and the two-dimensional frequency set $I_N = I_N^{\text{hc},0.9}$ for $N = 2, 3, \dots, 50$.

Hence, for the hyperbolic crosses $I_N^{\text{hc},\beta}$ with $\beta < \varepsilon$ we get the same error bound as in (7.4) for $\mathbf{c} = \mathbf{1}$. Generally, the choice of $\mathbf{c} > \mathbf{0}$ influences the rate of convergence. The fastest decay of the transformed Fourier coefficients in (7.6) is achieved for $c_j = 1$ and slows down for both $c_j \rightarrow 0$ and $c_j \rightarrow \infty$, resulting in worse approximation errors as seen in Figure 7.3 for $\mathbf{c} = \{\frac{4}{5}, \frac{9}{10}, \mathbf{1}\}$.

8 The construction of sparse frequency sets

Finally we want to make use of dimension incremental algorithms, the sparse fast Fourier transform (sparse FFT), see [15]. They reconstruct sparse multivariate trigonometric polynomials with an unknown support in a frequency domain I . Based on component-by-component construction of rank-1 lattices, the approach of [15, Algorithm 1 and Algorithm 2] describes a dimension incremental construction of a frequency set $I \subset \mathbb{Z}^d$ belonging to the non-zero or approximately largest Fourier coefficients. They restrict the search space to a full grid $[-N, N]^d \cap \mathbb{Z}^d$ of refinement $N \in \mathbb{N}$ and assume that the cardinality of the support of the multivariate trigonometric polynomial is bounded by a sparsity $s \in \mathbb{N}$. Then we end up with up to s non-zero Fourier coefficients of the respective test function. We were able to adapt these algorithms for transformed reconstructing rank-1 lattices and want to showcase the combination with the transformed lattice fast Fourier algorithms, see [11].

8.1 Example with algebraic transformation

For the algebraic transformation (4.1) with $\mathbf{c} = \mathbf{1}$ we already discussed the usage of multiple rank-1 lattices, see Figure 7.1. Previously the particular frequency set I_N was chosen to be a hyperbolic cross $I_N^{\text{hc},0.95}$, whereas now we let the sparse FFT algorithm determine a suitable frequency set. In dimension $d = 5$ and for each $N = 2, 3, \dots, 9$ we use the respective cardinality of hyperbolic crosses $|I_N^{\text{hc},0.95}|$ as the sparsity parameter s . Remarkably, the resulting approximation errors are just as good as the original discrete approximation error. On the other hand, even though the frequency sets have the same cardinality, the two-dimensional

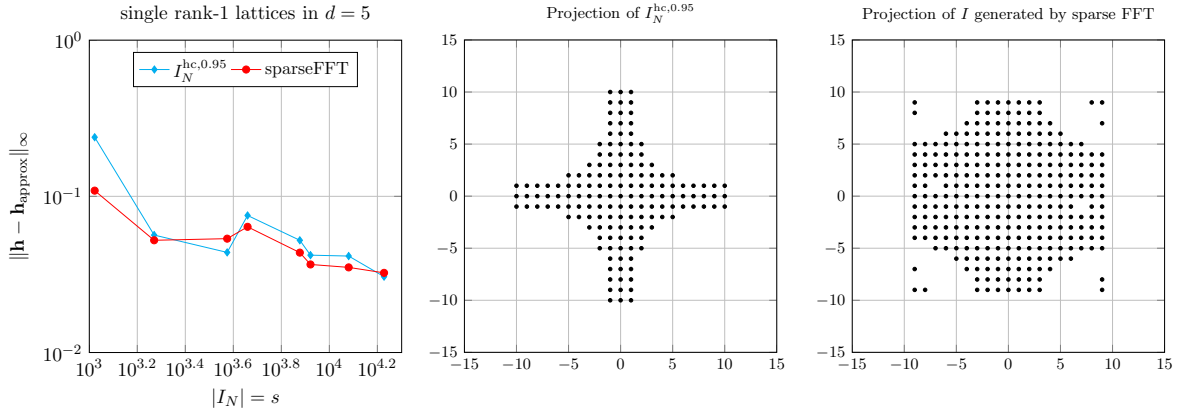


Figure 8.1: Relative discrete approximation error $\|\mathbf{h} - \mathbf{h}_{\text{approx}}\|_{\infty} / \|\mathbf{h}\|_{\infty}$ for single rank-1 lattices with the algebraic transformation for $I_N = I_N^{\text{hc},0.95}$ and I_N as the frequency set generated by the sparse FFT algorithm (left). Two-dimensional projections of $I_N^{\text{hc},0.95}$ (middle) and two-dimensional projection of the frequency set generated by the sparse FFT algorithm (right).

projections to their first two coordinates differ substantially in size and shape, as seen in Figure 8.1.

8.2 Example with the error and logarithmic transformation

The sparse FFT algorithm is especially interesting for the logarithmic transformation (4.2) and the error transformation (4.3), because we can't calculate the transformed Fourier coefficients (7.2) and thus can only hope to guess an frequency sets I that causes a small and linearly decaying approximation error for increasing $N \in \mathbb{N}$. Now we simply let the sparse FFT algorithm construct a suitable frequency set I depending on the sparsity $s \in \mathbb{N}$.

We return to dimension $d = 2$ and fix the refinement $N = 20$. Then the full 20×20 -integer grid contains $(2 \cdot 20 + 1)^2 = 1681$ elements. For the sparsities $s = 100$ and $s = 500$ both transformations lead to frequency sets I_N that strongly remind us of hyperbolic crosses, see Figure 8.2.

8.3 Example with the tangens transformation

Once again we consider the test function h as in (7.1) and the tangens transformation as defined in (4.4) with $\mathbf{c} = \mathbf{1}$. We already calculated the exact univariate transformed Fourier coefficients $\hat{h}_{k_j, \psi}$ in (7.3) and observed that they are non-zero only for $k_j \in \{-1, 0, 1\}$. Hence, over a full grid $[-N, N]^d \cap \mathbb{Z}^d$ with $(2N + 1)^d$ points there are just 3^d non-zero multivariate transformed Fourier coefficients $\hat{h}_{\mathbf{k}, \psi}$.

We check this for dimension $d = 12$ and $N = 4$ with the sparse FFT algorithm, see [15, Algorithm 2] and [20]. We initialize this algorithm with the transformed function $h(\tan(\pi \cdot))$, choose the algorithm name 'a2r1l' and set the sparsity parameter 'sparsity_s' to 10^6 . This results in an exact reconstruction as the algorithm indeed only detected the $3^{12} = 531441$ out of $(2 \cdot 4 + 1)^{12} \approx 2.8 \cdot 10^{11}$ possible frequencies, corresponding to the 12-dimensional integer unit cube of radius 1 for which the transformed Fourier coefficients are non-zero.

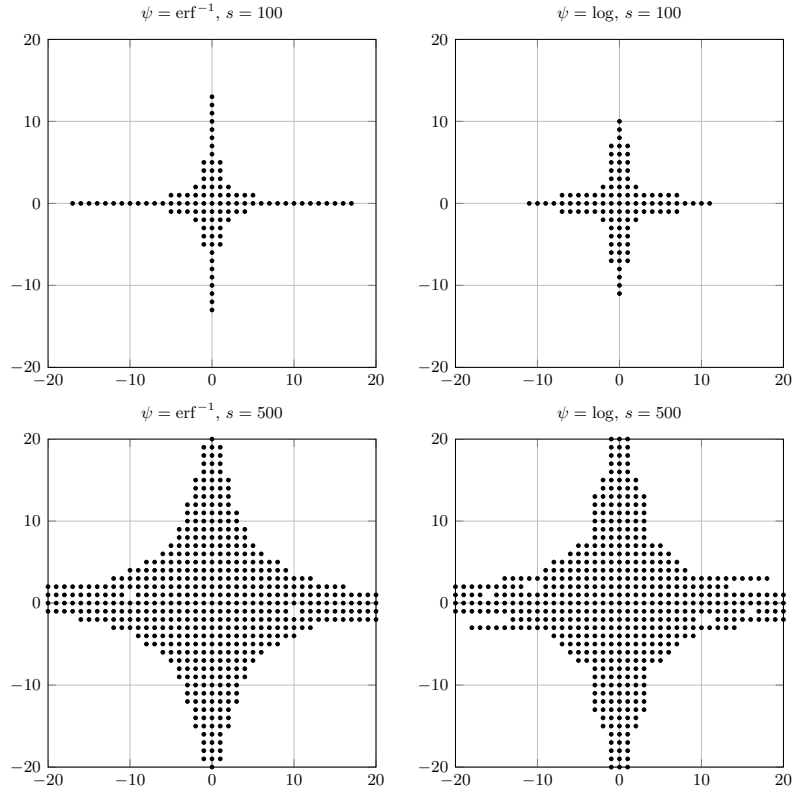


Figure 8.2: Two-dimensional frequency sets I_N with $N = 20$ and $s \in \{100, 500\}$ for the error and logarithmic transformation.

9 Conclusion

In this paper we discuss strategies for transforming functions over \mathbb{R}^d to the torus \mathbb{T}^d , such that we can use the known results for lattice rules on the torus. We discuss different transformations, transfer some approximation results presented in [10], develop the related algorithms and present numerical examples.

A single change of coordinate mapping $\psi : \mathbb{T}^d \rightarrow \mathbb{R}^d$ allows the extension of classical Fourier approximation methods for multivariate functions defined on the torus \mathbb{T}^d to functions defined on \mathbb{R}^d . In particular, algorithms based on single and multiple reconstructing rank-1 lattices can be adjusted for this new setting. Furthermore, the essential theoretical approximation error bound proposed in [6, Lemma 3.11.] remains valid for functions in the Wiener algebra $\mathcal{A}_{\psi, \omega}(\mathbb{R}^d)$. Remarkably, only slight modifications are necessary to incorporate the transformations into the algorithms for the evaluation and the reconstruction of transformed multivariate trigonometric polynomials presented in [6, Algorithm 3.1 and 3.2].

Our numerical tests reveal that these algorithms indeed yield a linear decay of the discretized approximation error. However, the actual rate of decay as well as the quality of the error are highly dependent on the choice of the frequency set I and the chosen parameter c . Dimension incremental construction methods for sparse frequency sets are also applicable and turn out to be a crucial tool when the Fourier coefficients of a test function can't be exactly evaluated.

Acknowledgements

The authors thank Lutz Kämmerer and Toni Volkmer for fruitful discussions during the preparation of this paper. Furthermore we thank Lutz Kämmerer to leave us the multiple lattice software, see [7, 8], and Toni Volkmer to leave us the software 'sparseFFTr1l' for computing the sparse fast Fourier transform based on reconstructing rank-1 lattices in a dimension incremental way, see [20]. The authors wish to express their gratitude to Holger Langenau for computing the integral (7.6). The first named author gratefully acknowledges the support by the funding of the European Union and the Free State of Saxony (ESF).

References

- [1] J. P. Boyd. *Chebyshev and Fourier Spectral Methods*. Dover Press, New York, NY, USA, second edition, 2000.
- [2] G. Byrenheid, L. Kämmerer, T. Ullrich, and T. Volkmer. Tight error bounds for rank-1 lattice sampling in spaces of hybrid mixed smoothness. *Numer. Math.*, 136:993–1034, 2017.
- [3] R. Cools, F. Y. Kuo, and D. Nuyens. Constructing lattice rules based on weighted degree of exactness and worst case error. *Computing*, 87:63–89, 2010.
- [4] R. Cools and D. Nuyens. Fast algorithms for component-by-component construction of rank-1 lattice rules in shift-invariant reproducing kernel Hilbert spaces. *Math. Comp.*, 75:903–920, 2004.
- [5] J. Dick, F. Y. Kuo, and I. H. Sloan. High-dimensional integration: The quasi-Monte Carlo way. *Acta Numer.*, 22:133–288, 2013.
- [6] L. Kämmerer. *High Dimensional Fast Fourier Transform Based on Rank-1 Lattice Sampling*. Dissertation. Universitätsverlag Chemnitz, 2014.
- [7] L. Kämmerer. LFFT, MATLAB[®] toolbox for the lattice and generated set based FFT. <http://www.tu-chemnitz.de/~lkae/lfft>, 2014.
- [8] L. Kämmerer. Constructing spatial discretizations for sparse multivariate trigonometric polynomials that allow for a fast discrete Fourier transform. *Appl. Comput. Harmon. Anal.*, 2017, accepted.
- [9] L. Kämmerer. Multiple rank-1 lattices as sampling schemes for multivariate trigonometric polynomials. *J. Fourier Anal. Appl.*, 24:17–44, 2018.
- [10] L. Kämmerer, D. Potts, and T. Volkmer. Approximation of multivariate periodic functions by trigonometric polynomials based on rank-1 lattice sampling. *J. Complexity*, 31:543–576, 2015.
- [11] L. Kämmerer, D. Potts, and T. Volkmer. High-dimensional sparse FFT based on sampling along multiple rank-1 lattices. *ArXiv e-prints 1711.05152*, 2017.
- [12] N. M. Korobov. On the approximate computation of multiple integrals. *Dokl. Akad. Nauk*, 124:1207–1210, 1959. In Russian.
- [13] F. Y. Kuo, G. W. Wasilkowski, and B. J. Waterhouse. Randomly shifted lattice rules for unbounded integrands. *J. Complexity*, 22(5):630–651, 2006.
- [14] H. Niederreiter. Quasi-Monte Carlo methods and pseudo-random numbers. *B. Am. Math. Soc.*, 84:957–1041, 1978.
- [15] D. Potts and T. Volkmer. Sparse high-dimensional FFT based on rank-1 lattice sampling. *Appl. Comput. Harmon. Anal.*, 41:713–748, 2016.
- [16] J. Shen, T. Tang, and L.-L. Wang. *Spectral Methods*, volume 41 of *Springer Ser. Comput. Math.* Springer-Verlag Berlin Heidelberg, Berlin, 2011.

- [17] I. H. Sloan and S. Joe. *Lattice methods for multiple integration*. Oxford Science Publications. The Clarendon Press Oxford University Press, New York, 1994.
- [18] I. H. Sloan and P. J. Kachoyan. Lattice methods for multiple integration: Theory, error analysis and examples. *SIAM J. Numer. Anal.*, 24:116–128, 1987.
- [19] V. N. Temlyakov. *Approximation of periodic functions*. Computational Mathematics and Analysis Series. Nova Science Publishers Inc., Commack, NY, 1993.
- [20] T. Volkmer. `sparseFFTr11`, MATLAB[®] toolbox for computing the sparse fast Fourier transform based on reconstructing rank-1 lattices in a dimension incremental way. <http://www.tu-chemnitz.de/~tovo/software>, 2015.
- [21] F. Weisz. Summability of multi-dimensional trigonometric Fourier series. *Surv. Approx. Theory*, 7:1–179, 2012.